

- 5 JUNI 1968

SPUTTERING OF F.C.C. METALS

INSTITUUT-LORENZ
voor theoretische natuurkunde
Nieuwsteeg 16-Leliden-Nederland

D. ONDERDELINDEN



SPUTTERING OF F.C.C. METALS

PROEFSCHRIFT

TER VERKRIJGING VAN DE GRAAD VAN DOCTOR IN
DE WETENSCHAP EN NATUURWETENSCHAPPEN AAN
DE RIJSHOOGESCHOOL TE LEIDEN, OP DRINGEN VAN
DE FACULTEIT WETENSCHAPPEN DE Z. HUNTERDIJK,
BIBLIOTHECAIR EN DE FACULTEIT DER GEWISSENSCHAPPEN,
TEN OVERSTAAN VAN EEN COMMISSIE UIT DE SAMEN
TE VERZAMLEN OP DONSDAG 21 MEI 1968
TE KLONK 11.30 UUR

DOOR

DIRK ONDERDELINDEN

GEBOREN TE ROTTERDAM IN 1940

INSTITUUT-L. G. B. 12
voor theoretische natuurkunde
Nieuwsteeg 12-Leyden-Nederland

1968 *kast dissertaties*

BRUNING-OFFSET ROTTERDAM

SPUTTERING OF FCC METALS

1968

SPUTTERING OF F.C.C. METALS

PROEFSCHRIFT

TER VERKRIJGING VAN DE GRAAD VAN DOCTOR IN
DE WISKUNDE EN NATUURWETENSCHAPPEN AAN
DE RIJKSUNIVERSITEIT TE LEIDEN, OP GEZAG VAN
DE RECTOR MAGNIFICUS DR. P. MUNTENDAM,
HOGLERAAR IN DE FACULTEIT DER GENEESKUNDE,
TEN OVERSTAAN VAN EEN COMMISSIE UIT DE SENAAT
TE VERDEDIGEN OP DINSDAG 21 MEI 1968
TE KLOKKE 15.15 UUR

DOOR

DIRK ONDERDELINDEN

GEBOREN TE ROTTERDAM IN 1940

INSTITUUT-LORENZ
voor theoretische natuurkunde
Nieuwsteeg 18-Leiden-Nederland

1968

BRONDER-OFFSET ROTTERDAM

PROMOTOR: PROF. DR J. KISTEMAKER

HOOGESCHOOL

DE VERENIGING VAN DE ONAAN DE DOCTOR IN
DE WETENSCHAP EN NATUURWETENSCHAPEN AAN
DE KUNSTEN EN WETENSCHAPEN IN LEIDEN, ONDER AAN
DE RECTOR MAGISTRUS DR. P. MOUTRIJN,
HOOGLERAAR IN DE FACULTEIT DER WETENSCHAPEN,
TE OVERSTAAAN VAN EEN COMMISSIE UIT DE RECTOR
TE VERBODEN OF ONTOEGANGELIJK OP 21 MEI 1964
TE KLOONEN 12 12 1964

1964

DEEL ONDERDELEN

Dit werk heeft gedeeltelijk plaatsgevonden onder de
leiding van Dr P.K. Rol.

The work in this thesis was part of the research program of the Stichting voor
Fundamenteel Onderzoek der Materie (Foundation for Fundamental Research
on Matter) and was made possible by financial support from the Nederlandse
Organisatie voor Zuiver-Wetenschappelijk Onderzoek (Netherlands Organisation
for the Advancement of the Pure Research).

PROF. DR. J. KISTEMAKER

FROM THE PROF. DR. J. KETEMEKER

THE AUTHOR

Dr. J. Ketemeker, born in 1892, studied at the University of Groningen, where he received his Ph.D. in 1920. He worked in the laboratory of Prof. Dr. J. van der Waals and later in the laboratory of Prof. Dr. J. van der Hoff. He is now a senior research fellow at the University of Groningen.

His research interests are in the field of physical chemistry, particularly in the study of the properties of gases and liquids. He has published several papers on these subjects in the *Journal of Physical Chemistry* and the *Journal of Chemical Physics*.

He is also a member of the Royal Netherlands Academy of Sciences and the Royal Society of London. He has been awarded several prizes and honors for his work, including the *Willemsfonds* prize in 1935 and the *Willemsfonds* prize in 1936.

He is currently working on a book on the properties of gases and liquids, which is expected to be published in the near future. He is also working on a number of other papers on related subjects.

His work has been published in the *Journal of Physical Chemistry* and the *Journal of Chemical Physics*. He is also a member of the Royal Netherlands Academy of Sciences and the Royal Society of London.

The work in this thesis was part of the research program of the Scientific Year Fundamentals of Chemistry of the Netherlands (Fonds voor Fundamenteel Wetenschappelijk Onderzoek) and was made possible by financial support from the Nederlandse Organisatie voor Wetenschappelijk Onderzoek (Netherlands Organization for Scientific Research).

STELLINGEN

I

Als men een vaste stof beschiet met ionen worden Frenkelparen gecreëerd. Het is interessant en mogelijk het aantal, dat de verstuiwingsverhouding kan beïnvloeden, te berekenen.

J. B. Sanders; proefschrift, Leiden, 1968.

II

Het optreden van de minima in de verstuiwingsverhouding juist naast de open richtingen, zoals voorspeld in het transparantiemodel van Southern c. s., is te wijten aan tekortkomingen van het model.

A. L. Southern, W. R. Willis en M. T. Robinson, *J. Appl. Phys.* 34, 153 (1963).

M. T. Robinson en A. L. Southern, *J. Appl. Phys.* 38, 2969 (1967).

Dit proefschrift, hoofdstuk IV, fig. 4.1.

III

Het model van Lehmann en Sigmund geeft een fraaie verklaring voor het optreden van voorkeursuittreedrichtingen voor verstoven atomen. Het aantal atoomlagen dat een rol speelt in dit model is echter essentieel groter dan twee en vormt daarom geen ondersteuning van het model van Harrison c. s.

C. Lehmann en P. Sigmund, *Phys. Stat. Sol.* 16, 507 (1966).

D. E. Harrison, J. P. Johnson en N. S. Levy, *Appl. Phys. Lett.* 8, 33 (1966).

IV

De conclusie van Johnson c. s., dat aan het criterium van Hanes over de lengte van de buisjes in een Zacharijsoven, ter verkrijging van moleculaire bundels, de voorkeur moet worden gegeven boven het criterium van Giordmaine en Wang, wordt door hun metingen niet gerechtvaardigd.

J. C. Johnson, A. T. Stair Jr. en J. L. Pritchard, *J. Appl. Phys.* 37, 1551 (1966).

G. R. Hanes, *J. Appl. Phys.* 31, 2171 (1960).

J. A. Giordmaine en T. C. Wang, *J. Appl. Phys.* 31, 463 (1960).

V

Aan de juistheid van de metingen van Sterk c. s. over emissie van zachte röntgenkwanten tengevolge van bombardement van vaste stoffen met ionen in het keV energiegebied mag getwijfeld worden op grond van metingen van het inelastisch energieverlies bij botsingen tussen atomen.

A. A. Sterk, C. L. Marks en W. P. Saylor, *Adv. in X-ray Analysis*, Vol. X, Plenum Press, New York, 1967, p. 399.
C. Snoek, W. F. van der Weg, R. Geballe en P. K. Rol, *Physica* 35, 1 (1967).

VI

De conclusie van Bell c. s., dat de Born benadering voor de aanslag van n^1D niveaus in He door protonen geldt voor energieën van 50 keV en hoger, is onjuist.

K. L. Bell, D. J. Kennedy en A. E. Kingston, J. Phys. B (proc. Phys. Soc.) 2, 218 (1968).

VII

Het bepalen van werkzame doorsneden voor "electronenvangst" van meervoudig geladen ionen kan zeer goed worden uitgevoerd via een onderzoek naar de ladings-toestand van aan gas gestrooide ionen. Men variëert daartoe de druk van het gas.

VIII

Hoffman behandelt een calibratieapparaat voor drukmeters gebaseerd op de zogenaamde continue-stroom methode. Zijn bewering dat dit apparaat een nauwkeurigheid heeft van 4% in het drukgebied van 2×10^{-6} tot 10^{-3} torr is aanvechtbaar.

V. E. Hoffman, Research/Development Magazine, April, 1963.

IX

Voor het beschrijven van het vacuum wordt ten onrechte het begrip druk gebruikt en niet de dichtheid.

X

In de theorieën over kinetische secundaire electronenemissie van Parilis c. s. en van Harrison c. s. wordt, ongemotiveerd, de bijdrage van respectievelijk projectielelectronen en doelwitelectronen verwaarloosd.

E. S. Parilis en L. M. Kishinevskii, Soviet Physics-Solid State 3, 885 (1960).

D. E. Harrison Jr., C. E. Carlston en G. D. Magnuson, Physical Review 139, A737, (1965).

2.3.2. The scattering ratio as a function of the angle of incidence	32
CHAPTER III. Theory of collisions in a crystal lattice	35
3.1. Introduction	35
3.2. The interaction potential	36
3.3. Forward collisions	42
3.4. Channeling of the incident ions	45
3.4.1. Theory of Lindhard	47
3.4.2. Theory of Lohmann	48

VOORWOORD

Teneinde te voldoen aan de wens van de Faculteit der Wiskunde en Natuurwetenschappen volgt hier een kort overzicht van mijn studie.

In 1957 behaalde ik het einddiploma H. B. S. -B aan Het Charlois Lyceum te Rotterdam, waarna mijn inschrijving aan de Rijksuniversiteit te Leiden volgde. In 1960 deed ik kandidaatsexamen in de Wiskunde en Natuurwetenschappen (A'). Daarna werkte ik op het Kamerlingh Onnes Laboratorium. Onder leiding van dr Z. Dokoupil werden metingen van de soortelijke warmte van antiferromagnetische zouten in het temperatuurgebied van 1^oK tot 30^oK uitgevoerd.

In 1963 legde ik met goed gevolg het doctoraalexamen af, met experimentele natuurkunde als hoofdvak en klassieke mechanica als bijvak.

Inmiddels had ik mijn werkterrein verlegd naar het FOM Instituut voor Atoom- en Molecuulfysica te Amsterdam, onder directie van Professor dr J. Kistemaker. De in dit proefschrift beschreven experimenten werden aldaar verricht onder leiding van dr P.K. Rol.

CONTENTS

	page
CHAPTER I. Survey of experimental and theoretical work on sputtering.	11
1.1. Introduction	11
1.2. Methods for producing the incident ions	12
1.3. Determination of the sputtering ratio S	13
1.4. Some experimental results	14
1.4.1. Energy dependence of the sputtering ratio for normally incident ions	14
1.4.2. The angular dependence of the total sputtering ratio	15
1.4.3. The angular- and velocity distribution of sputtered particles	17
1.5. Theory	19
CHAPTER II. Description and results of the experiments.	23
2.1. Introduction	23
2.2. Experimental remarks	23
2.2.1. The ion beam	23
2.2.2. Surface condition	24
2.2.3. Vacuum system	26
2.2.4. The target holder	27
2.2.5. Determination of the sputtering ratio S	28
2.2.6. Accuracy of the measured sputtering ratio	28
2.3. Experimental results	29
2.3.1. The sputtering ratio as a function of the energy for normally incident ions	29

	page
2.3.2. The sputtering ratio as a function of the angle of incidence	32
CHAPTER III. Theory of collisions in a metal lattice.	39
3.1. Introduction	39
3.2. The interaction potential	39
3.3. Focusing collisions	43
3.4. Channeling of the incident ions	45
3.4.1. Introduction	45
3.4.2. Theory of Lindhard	46
CHAPTER IV. Theory of sputtering and comparison with the experimental results.	50
4.1. Introduction	50
4.2. Transparency theories	51
4.2.1. Theory of Southern, Willis and Robinson	51
4.2.2. Theory of Magnuson and Carlston	54
4.2.3. Theory of Odintsov	56
4.3. The influence of channeling on single crystal sputtering	62
4.3.1. Extension of the hard sphere transparency model	66
4.3.2. Description of the experimental results with a power potential	68
REFERENCES	80
SUMMARY	83
SAMENVATTING	85

CHAPTER I

SURVEY OF EXPERIMENTAL AND THEORETICAL WORK ON SPUTTERING

1.1. INTRODUCTION

One of the effects observed as a result of ion bombardment of solids is sputtering. Much work has been devoted to this special phenomenon in recent years. The increased interest in the subject rises among other reasons from the importance of the effect in the field of radiation damage, space research, plasma physics, surface conditioning, ion getter pumps, electrode erosion in gas-discharge tubes, the deposition of thin layers of metals and in general the interaction of fast particles with atoms in a solid.

Since the sputtering effect was first reported, about a century ago, many attempts have been made to give a theoretical explanation of the experimental results. But during a long time there were not many reliable data available. This was mainly due to the poor experimental conditions under which, until about 10 years ago, the measurements were performed.

Information about the sputtering process can be obtained from measurements of the total sputtering ratio, i. e. the number of atoms ejected per incoming ion. Basic parameters involved are the ion energy, type of the incident ion, angle of incidence, material to be sputtered, target temperature, surface condition and if single crystals are used the orientation of the exposed crystal face. Other information about sputtering can be obtained from the angular and velocity distribution of the sputtered atoms. One can distinguish between so-called "physical" and "chemical" sputtering. Chemical sputtering arises whenever a reactive ion and the target material form volatile compounds. Physical sputtering on the other hand is caused by a collision process between incident ion and lattice atom. For an in-

vestigation of the fundamental processes in the sputtering phenomenon however one must, to avoid any chemical influence, take combinations of incident ion and target material which do not make a stable compound at all.

In the following sections we will give a description of the experimental techniques and some of the results obtained. The last section of this chapter is a short review of some theories.

1.2. METHODS FOR PRODUCING THE INCIDENT IONS

The oldest and simplest way of observing sputtering was in the glow discharge (Grove, 1852). The sputtering occurs at the cathode as a consequence of which this phenomenon was given the name "cathode sputtering". Numerous qualitative data have been obtained with the glow discharge method (see for instance the review article of Wehner, 1955). Quantitative information concerning the influence of the above mentioned parameters cannot be obtained with this method. The relatively high pressure (higher than 0.1 Torr) causes an enormous spread in energy and angle of incidence of the ions striking the surface and a back diffusion to the surface of the sputtered particles. By introducing a magnetic field the pressure could be reduced to 10^{-2} Torr and more reliable data could be obtained (Penning and Moubis, 1940). However, the ions still have a wide range of energies. Furthermore it is difficult to determine the angle of incidence of the projectiles.

At pressures of the order of 10^{-3} Torr the problems mentioned above could be eliminated. At these pressures it is only possible to maintain a discharge with a thermionic or a pool type cathode (Wehner, 1955). In this method the energy of the ions can be determined sufficiently accurate. For target dimensions large compared with the thickness of the Langmuir sheath surrounding it, the ions impinge on the target along the surface normal. Current densities can be made high enough to prevent surface contamination. A disadvantage of this method is that it is not possible to measure the secondary electron emission from the target. Thus the measured current is too high and as a result the experimental sputtering ratios are too low.

In recent years most investigations have been carried out with ion beams. Ions are extracted from a plasma and then accelerated and focused onto a target (for instance Yurasova et al., 1960). In this method the secondary electron emission can be suppressed or measured. With the ion beam method it is possible to study the dependence of the sputtering ratio on the angle of incidence of

the bombarding ions. Furthermore, by using a mass analyser it is possible to bombard the target with ions of one mass over charge ratio (Yonts et al., 1958, Rol et al., 1957).

The main problem in this method is formed by the low current densities at the target as a consequence of which the sputtering rate is too low to prevent the formation of an oxide layer. However, recent development of high intensity ion sources and the possibility of reaching a good vacuum around the target have made reliable measurements possible.

1.3. DETERMINATION OF THE SPUTTERING RATIO S

A common way to determine the number of sputtered particles per incoming ion is to measure the weight loss, M of the target as a result of an incident ion current I during a time t . The sputtering ratio can then be calculated from the relation:

$$S = N e M / A I t \quad (1.1)$$

where A is the atomic weight of the target atoms, e the charge of an incoming ion and N the number of Avogadro. There are several effects which can influence the value of M . The ions impinging on the target may be captured in the lattice and increase the weight of the target by an amount m_1 . The weight measurements are usually carried out in air and adsorption layers developed on the target surface cause an uncertainty m_2 . In most cases the experiments are performed in such a way that $M \gg m_1, m_2$.

Another possible way of determining the number of sputtered particles is provided by the use of a collector. The amount of condensed material can be determined by measuring the increase in weight of the collector. This amount can also be determined by activation of the sputtered material or by bombarding a target which contains a radioactive isotope and measuring the activity of the collector. A disadvantage of these methods is the possibility that not all the sputtered particles will condense on the collector.

In the experimental arrangement where the target is immersed in a plasma the sputtering ratio can be found by measuring the intensity of an emission line of the target particles excited in the plasma. In the ion beam method, which is used for the measurements described in this thesis, excitation of the sputtered particles can be achieved in an electron beam in front of the target. Using a monochromator and a photomultiplier an emission line can be observed. The

spread in the velocity and angular distribution of the sputtered atoms for different bombarding directions of ions on single crystals gives rise to unequal excitation probabilities, introducing uncontrollable errors in the measured sputtering ratio.

1.4. SOME EXPERIMENTAL RESULTS

It is not the purpose of this section to give an extensive survey of all the work done in sputtering. This can be found in extensive review articles on sputtering by Behrisch (1964) and by Kaminski (1965). In this section the typical dependence of the sputtering ratio on parameters like energy and mass of the projectile, angle of incidence and exposed crystal orientation will be shown. Besides that some remarks about the angular and velocity distribution of the sputtered particles will be made. Most of the discussed sputtering measurements have been performed with the ion beam method.

1.4.1. Energy dependence of the sputtering ratio for normally incident ions

The general behaviour of the sputtering ratio for a given ion-target combination can be described in the following way: the sputtering ratio increases from threshold (in the order of 10 eV) roughly as E^2 , which dependence gradually changes into a linear increase with energy. This linear part is followed by a broad maximum, the place of which depends strongly on the mass of the impinging ions. For still higher energies a decrease with ion energy is observed. For the very light ions as H^+ and He^+ the constant part is found at a few keV and the sputtering yield is much less than 1 atom per ion. For heavy elements like Xe^+ the constant part of the yield is found in the 100 keV region and the yield is more than 10 atoms per ion. In the low energy region most of the results come from Wehner et al. (1956, 1957, 1958). For the higher energies the work of Rol (1960), Yonts et al. (1960), Perovic (1961) and especially Almèn and Bruce (1961) should be mentioned. An illustration of the typical energy dependence of the sputtering ratio is given in fig. 1.1 for different projectiles on polycrystalline copper. It can be seen that the energy at which the maximum of the sputtering is reached decreases with the mass of the bombarding ion. Furthermore it appears that for energies well above threshold the sputtering ratio increases with increasing mass of the projectile. In the region near threshold the

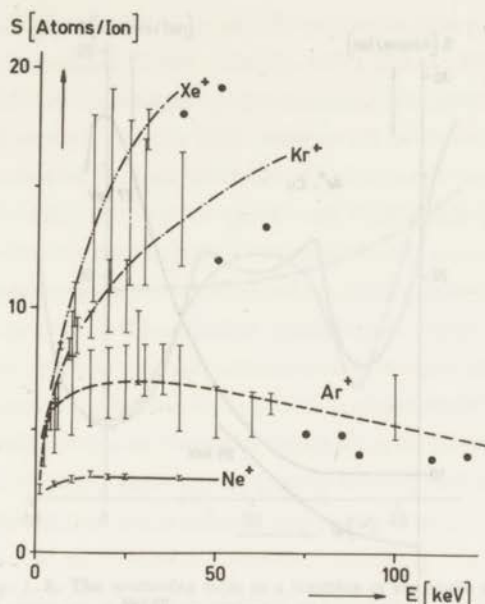


Fig. 1.1. The sputtering ratio of polycrystalline copper under normally incident noble-gas ion bombardment. (see Behrisch, 1964).

behaviour is more complicated, but we will not go into detail about this region.

The results on monocrystalline targets are not as extensive as for polycrystalline material. However, it can be supposed that the results of Southern et al. (1963), Magnuson et al. (1963) and more recently Snouse et al. (1966) for Ar^+ ions on (100), (110) and (111) Cu crystals give the general behaviour for the energy dependence of the sputtering ratio for normally incident ions on f.c.c. single crystals. First of all it can be observed that the maxima occur at a lower energy as in the polycrystalline case (fig. 2.3). Furthermore the maximum in the $S(E)$ curve is found at slightly different energies for the three crystal faces. The explanation of these characteristics will be discussed in more detail in chapter IV. It may be remarked that the ratios $S_{(111)}/S_{(100)}$ and $S_{(110)}/S_{(100)}$ do not remain constant in the energy range studied.

1.4.2. The angular dependence of the total sputtering ratio

In measuring the angular dependence of the sputtering ratio it has been found that for oblique incidence of the ions the yield is higher than for normal

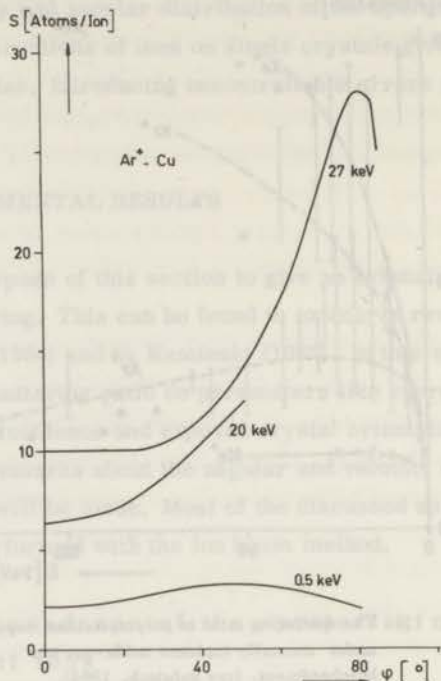


Fig. 1.2. The sputtering ratio as a function of the angle of incidence for Ar^+ ions on polycrystalline copper (Molchanov, 1961, Rol, 1959 and Wehner, 1959).

incidence of the ions. Fig. 1.2 shows some results. It can be seen that for higher energies the sputtering ratio is more sensitive for a change in the angle of incidence. It is not possible to deduce from the angular measurements made so far a systematic behaviour of the sputtering ratio for different ion-target combinations (see also Dupp et al., 1966). For monocrystalline targets a more complicated behaviour has been observed. The sputtering yield depends on the "transparency" (Fluit et al. 1963) of the crystal in the direction of the ion beam. In the transparent direction the sputtering yield is low, whereas in the opaque direction the yield is relatively high. In Fig. 1.3 measurements of Molchanov (1961) and Rol (1959) are shown. For this case minima occur at the $[100]$ and $[211]$ -direction. Measurements of $S(\varphi)$ vs φ described in this thesis have been performed to analyse the influence of lattice parameter, mass and energy on the behaviour of the $S(\varphi)$ curve.

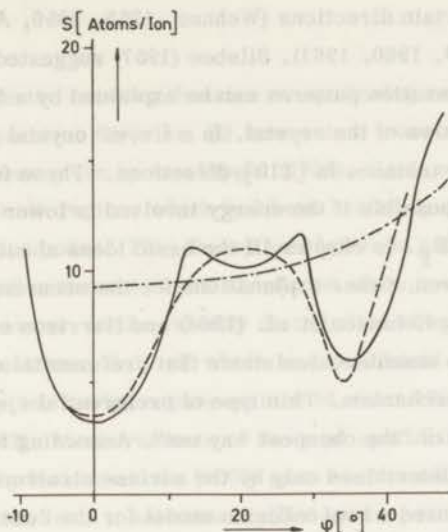


Fig. 1.3. The sputtering ratio as a function of the angle of incidence for Ar^+ ions on (100) Cu. The angle of incidence is changed by rotating the crystal around a $[011]$ direction in the surface.

- Rol (1959), 20 keV
- - - Molchanov (1961), 27 keV
- · - Molchanov (1961), 27 keV Ar^+ ions on polycrystalline copper.

1.4.3. The angular- and velocity distribution of sputtered particles

For energies near threshold most sputtered particles are found in the specular direction of the incoming ion beam. For normally incident ions a symmetrical distribution with a "dip" along the surface normal has been found. This "dip" gradually disappears for increasing energy of the incident ions (Wehner, 1960). The angular distribution of sputtered particles for incident ions in the keV region is found to be symmetrical around the surface normal and independent of the angle of incidence of the ions (Cobić and Perović 1959, Rol et al., 1960, Patterson et al., 1962). Some authors however have found a relative maximum in a direction making an angle of about 80° with the incident beam direction (Grönlund and Moore, 1960, Viehböck, 1967). This relative maximum can perhaps be correlated with direct momentum transfer (Fluit, 1963) to a surface atom. Particles sputtered from a monocrystalline surface are emitted

preferentially in certain directions (Wehner, 1955, 1956, Anderson and Wehner, 1960, Koedam, 1959, 1960, 1961). Silsbee (1957) suggested that the observed "spots" in the condensation patterns can be explained by a focusing mechanism in the closepacked rows of the crystal. In a f. c. c. crystal this focusing mechanism can occur for instance in $[110]$ -directions. These focused collision sequences are only possible if the energy involved is lower than a certain limit, the focusing energy E_F . In chapter III the basic ideas about such "correlated" collisions will be given. Other explanations for the occurrence of preferential ejection are given by Robinson et al. (1964) and Harrison et al. (1966). Robinson found from machinecalculations that preferential ejection can occur without a focusing mechanism. This type of preferential ejection seems to be based on a principle of "the cheapest way out". According to Harrison the preferential ejection is determined only by the surface structure. Lehmann and Sigmund (1966) proposed a two-collision model for the description of spot patterns. It follows from all these different points of view that the discussion about this subject is still going on.

Investigations to determine the mean energy and the energy distribution of the sputtered particles are of great interest for a better understanding of the collision processes important for sputtering. For incident ions in the low energy region mean velocities of sputtered particles from polycrystalline targets have been measured by Wehner (1959). From the force exerted on a quartz spring balance by the sputtered atoms the mean velocity could be calculated. The corresponding mean energy lies in the order of 10 eV for bombarding energies in the order of 500 eV. This high value was an item against an evaporation theory for sputtering. Almèn and Bruce (1961) found values in the order of 40 eV for polycrystalline materials under 35 keV Xe^+ ion bombardment, using a calorimetric method. Similar results have been obtained by Kopitzki and Stier (1961, 1962) for a great variety of metals. Mean energies of particles ejected from f. c. c. crystals have been studied with a calorimetric method by Weysenfeld (1966, 1965) in the low energy region. A relative minimum in the mean energy was found for particles ejected along the close packed directions in the crystal.

The velocity distribution of particles ejected from monocrystalline targets has been measured by various authors (Thompson, 1963, Stuart et al., 1962, 1964, Beuscher and Kopitzki, 1965). Several authors claim that from their measured velocity distribution the focusing energy E_F can be deduced.

1.5. THEORY

For many years the existing theories on sputtering could be divided into two groups: (a) evaporation theories; (b) momentum transfer theories. The first evaporation theory was given by von Hippel (1926). He described sputtering as evaporation from small regions which had been heated by the incident particles, well above the melting point. This theory was later-on extended by Townes (1944). The evaporation theories were abandoned since more experimental data came available. However, in the velocity distribution of sputtered gold atoms there was found a peak near 0.15 eV which was consistent with a theory of evaporation from a hot spike, having a temperature of about 1750°K (Thompson, 1961, Kopitzki et al., 1962). Measurements of the total sputtering ratio performed at high temperatures by Nelson et al. (1965) gave results which also can be explained by evaporation from a hot zone created by the primary particle. It was found, for polycrystalline materials, that the sputtering ratio was independent of the temperature up to a certain critical temperature where a sharp increase was found. This is due to the fact that the spike will remain at a high enough temperature to emit atoms by evaporation during a longer time when the crystal is at a higher temperature. The number of particles emitted by this mechanism depends on the initial spike radius, the conduction of heat to the lattice and the heat of vaporization. The spike temperature is a direct function of its radius if we suppose that all the primary energy goes into the spike. The theoretical curves could be fitted to the experimental results by making the right choice for the radius and the heat conduction to the lattice. The spike size depends on the cross-section for secondary collisions, the atomic density and the efficiency for focusing collisions. The spike dimensions (of the order of 100 \AA in gold) deduced from the experimental results are in qualitative agreement with what one should expect from these parameters. Quite generally one can say, however, that the evaporation from thermal spikes is important only for some special cases.

In the momentum transfer theories it is supposed that the energy transfer takes place through two particle collisions. This is only true when the interaction potential drops fast enough to give a negligible overlap with the interaction potential of the neighbouring atoms for the collision considered. Furthermore the amount of energy transferred has to be well above the binding energy. The first momentum transfer theory was given by Kingdom and Langmuir (1923), more sophisticated theories have been given by Keywell (1955) and Harrison (1956, 1957, 1960). An objection against these theories is the approximation of

an energy-independent collision cross-section. Several treatments have been given for sputtering by highly energetic protons, deuterons and helium ions (Goldman and Simon, 1958, Pease, 1960, Thompson 1961). These treatments can only be applied for the case where the collision cross-section is very small and are therefore restricted to the cases mentioned above. A more extensive treatment therefore will not be given. For lower energies and heavier ions the situation is much more complicated because the displaced atoms are not far apart and also the energy transferred to the target atoms is much higher than for the light ion case. More collision cascades originating from one primary atom can contribute to sputtering. For this case most theories are semi-empirical.

A mean free path theory has been proposed by Rol et al. (1960). In this theory it is assumed that only the first collision of the incident ion with the target atoms near the surface contributes to the sputtering process. The mean energy transferred in a collision is proportional to $M_1 M_2 E / (M_1 + M_2)^2$, where M_1 and M_2 are the mass of the incident ion and target atom respectively and E the energy of the incident ions. If one assumes the sputtering ratio to be proportional to the mean transferred energy in the first collision and inversely proportional to the depth of this collision below the surface one can put

$$S(E, \varphi) = K \frac{M_1 M_2}{(M_1 + M_2)^2 \lambda(E) \cos \varphi} E \quad (1.2)$$

where $\lambda(E)$ is the mean free path of the incident ions, φ the angle of incidence with respect to the surface normal and K a proportionality constant. For the calculation of $\lambda(E)$ the exponentially screened Coulomb potential was used. With this potential a hard sphere radius R can be defined with the aid of the equation

$$E = \left((M_1 + M_2) / M_2 \right) V(R) \quad (1.3)$$

and $\lambda(E)$ is then given by

$$\lambda(E) = (N \pi R(E)^2)^{-1} \quad (1.4)$$

where N is the number density of the target.

The formula mentioned above has been extended by Almèn and Bruce (1961),

putting $K = \beta \exp - \left[\frac{bM_1 E_B}{M_1 + M_2} \right]$, where β and b are universal constants and E_B the surface binding energy. Despite the rather crude assumptions, the predictions of this model are in fair agreement with the experimental sputtering ratios for ions on different metals in the keV region.

It was pointed out by Fluit (1963) that this mean free path theory also could be used for the description of sputtering results of monocrystals. This idea was worked out by various authors (Southern et al., 1963, Magnuson et al., 1963, Odintsov, 1963 and Martynenko, 1965) as will be treated in chapter IV.

Interesting is also a theory for normally incident ions on monocrystals (Lehmann, 1965). This theory is based on a hard sphere model and uses also the mechanism of focused collision sequences. The first collision of an incident ion is treated in detail. The collision products are assumed to collide again, and to lose all their energy, after one mean free path. This means that after the first collision the crystal is assumed to consist of randomly distributed atoms. All sputtered particles are assumed to be ejected as a result of focusing collisions. The number of recoil atoms that can start a focused collision sequence and the range of such a sequence have been calculated with a hard-sphere approximation given by Leibfried (1959). The focused collision sequences are assumed to start at the, above defined, end points of the collision products of the first collision. In this way the number of particles ejected can be calculated without fitting parameters. A surprisingly good qualitative description for the energy dependence of the sputtering ratio is obtained for the case of normally incident Cu^+ ions on (111)-, (110)- and (100) Cu crystals in the keV region. In this theory use have been made of very long ranges for focused collision sequences, in contradiction with calculations of Sanders et al. (1964) and Nelson et al. (1962). The effect of these long ranges is probably compensated by the used hard-sphere approximation for the incoming ions, giving a cross-section which is too small.

This model has been extended by Sanders et al. (1966) using a more realistic potential model for the first collision of the incoming ion. This first scattering has been treated with the help of the numerical results obtained by Robinson (1963) for the Thomas-Fermi potential. After the first scattering the lattice was considered to be a random arrangement of hard spheres. With a method, given by Leibfried (1963) the average location and dimensions of the collision cascades, caused by the products of the first collision were calculated. The recoil atoms were supposed to be homogeneously distributed throughout the

cascade volume. The number of focused collision sequences, originated by the recoil atoms in the cascade have been calculated with a hard-sphere approximation (Leibfried, 1959). For the range of such sequences the calculations of Sanders et al. (1964), for room temperature, were used. In this way the sputtering ratio for normally incident Ar^+ ions on (111)-, (110)-, and (100) Cu crystals has been calculated for projectile energies between 5 and 25 keV. The results are quite satisfactory for the (110) and (100) surfaces and about 20% too low for the (111) surface. This is presumably due to the wrong orientation dependence of this treatment (see Chapter IV). A weak point in this theory is the calculation of the energy distribution of the recoil atoms. This energy distribution has been calculated with a hard-sphere model. It has been shown later (Sanders, 1966) that calculations of the energy distribution of recoil atoms with the aid of a power potential lead to a strong dominance of very low energetic recoils. This in contrast with the hard-sphere model where the distribution function is independent of the recoil energy.

In spite of the fact that theories mentioned above describe some experimental results rather good, it is clear that still many aspects are not yet understood. The following subjects can be mentioned in this respect: the influence of the length of focused collision sequences on the magnitude of the sputtering ratio, the number of collisions of the incident ions contributing the sputtering and the influence of the channeling mechanism on the sputtering yield.

It can be concluded that, although there is much progress, more work have to be done, experimentally and theoretically, to clarify the sputtering phenomenon.

CHAPTER II

DESCRIPTION AND RESULTS OF THE EXPERIMENTS

2.1. INTRODUCTION

Reproducible measurements of the sputtering ratio S depend, besides a sufficiently accurate knowledge of the parameters which were discussed in Chapter I, on a reliable measurement of the number of ions striking the surface and the resulting number of sputtered atoms. Furthermore it is necessary that the measurements are performed on a smooth and atomically clean surface. With an electromagnetic isotope separator these requirements can be fulfilled rather simply, as will be discussed below, and this type of machine can therefore be regarded as a good tool for doing sputtering measurements.

An extensive description of the machine used for the experiments which are described in this thesis has been given by Zilverschoon (1954). It is therefore sufficient to confine the discussion to experimental circumstances around the target.

It may be remarked here that the energy range available with the 180° Amsterdam isotope separator has been extended to an energy of 45 keV, by the installation of an ion source of the same type as described by Rol in his thesis (1960).

2.2. EXPERIMENTAL REMARKS

2.2.1. The ion beam

The 180° isotope separator gives us at the collector side an ion beam con-

sisting of ions with one mass-over-charge ratio. Typical intensities for Ar^+ ions of 5 keV and 45 keV were $20 \mu\text{A}/\text{cm}^2$ and several hundreds of μA per cm^2 respectively. The angular spread, determined by diaphragms is 3° in the horizontal plane and 0.2° in the vertical plane. A smaller angular spread, which is desirable, could not be used because the resulting decrease in intensity could not be accepted (section 2.2.3). However, the rather smooth behaviour of the $S(\varphi)$ vs φ curve - where φ is the angle of incidence with respect to the surface normal - keeps the inaccuracy, in the measured sputtering ratio due to the angular spread of 3° , within 2%. The target used for the sputtering measurements is placed on the focusing point of the separator and a circular diaphragm with an area of about 1 cm^2 is placed in front of it. The radius R of the half circular orbits of singly charged ions is given by $R = \frac{1}{B} \sqrt{\frac{2MV}{e}}$, in which B is the magnetic induction, V the accelerating voltage, M the mass of the ions and e the elementary charge. The maximum possible energy spread of the ions reaching the target can now be given by $\frac{\Delta E}{E} = 2 \frac{\Delta R}{R}$, where the energy E is equal to eV . In our configuration we have $R = 100 \text{ cm}$ and $\Delta R \approx 0.25 \text{ cm}$, so $\frac{\Delta E}{E} = 0.5 \%$. The resulting inaccuracy in the sputtering ratio is less than 0.1%.

2.2.2. Surface condition

The sputtering ratio is determined by the interaction of an incoming ion with a small region of the target near the surface. It is therefore obvious that surface layers, formed by adsorption or chemical bond, will have a strong influence on the value of the measured sputtering ratio. To prevent the formation of surface layers the sputtering rate must be made an order of magnitude higher than the sticking rate of background gas molecules. The ion beam has the lowest intensity at 5 keV, namely about $20 \mu\text{A}/\text{cm}^2$. The lowest sputtering ratio for that energy is about 3 atoms/ion, so the minimum number of sputtered target atoms per cm^2 per second is about $4 \times 10^{14}/\text{cm}^2 \text{ s}$. The number of molecules N of the surrounding gas reaching the target per second per cm^2 is given by $N = \frac{1}{4} n \bar{v}$, where n is the number density per cm^3 of gas molecules and \bar{v} their mean velocity in cm per second. The molecules in the background gas, with the highest sticking probability, are oxygen, nitrogen and water molecules. Their sticking probability on the used targets is of the order of one half. At room temperature the mean velocity of these molecules is of the order of $5 \times 10^4 \text{ cm/s}$ and a sticking rate of $0.2 \times 10^{14}/\text{cm}^2 \text{ s}$, 5% of the sputtering rate, occurs for a density of $3 \times 10^9/\text{cm}^3$.

The corresponding partial pressure is 7×10^{-8} Torr. So for a total partial pressure of oxygen, nitrogen and water vapour lower than 7×10^{-8} Torr and current densities higher than $20 \mu\text{A}/\text{cm}^2$, the surface covering of impurity gas atoms is less than 5 %. This low cover percentage certainly reduces the fault in the absolute sputtering ratio to less than 1 %.

The surface is made as smooth and faultless as possible by electroplishing the single crystalline targets before each bombardment (see for instance Tegart, 1959). For this electropolishing procedure a Disa Electropol (see Fig. 2.1) with some small modifications has been used. After a number of bombardments the

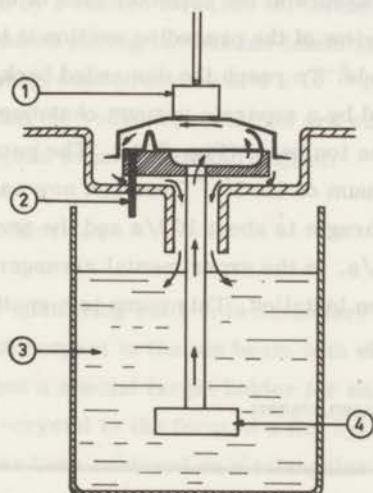


Fig. 2.1. Schematic view of the used electropolishing apparatus (Knuth System, Struers, Copenhagen).
1 Crystal (anode), 2 Cathode, 3 Electrolyte, 4 Pump.
The direction of the liquid flow is indicated by arrows.

surface of the target is made flat again by mechanical polishing. In this case the electropolishing should be long enough to remove the deformation layer, formed during the mechanical polishing.

The surface temperature of the target effects the sputtering ratio. However, measurements of Nelson (1962) and of Magnuson and Carlston (1965) have shown that this influence is weak in the temperature region far from the melting point of the target. In fact no change in the sputtering ratio for polycrystalline targets has been found for temperatures more than 200° from the melting tem-

perature. Magnuson and Carlston have found small changes (1 % per 100 °K) in the sputtering ratio of monocrystalline copper targets for temperatures between 300 °K and 800 °K. It is therefore sufficient to limit the target temperature by cooling with a constant flow of water. The temperature of the target during our measurements ranges from 290 °K to 330 °K depending on the energy input per second. The inaccuracy in the sputtering ratio due to this temperature fluctuation can be neglected.

2.2.3. Vacuum system

The background pressure at the collector side of the separator is of the order of 10^{-6} Torr. In view of the preceding section it is clear that extra vacuum provisions had to be made. To reach the demanded background pressure, the target has been enclosed by a separate vacuum chamber with a small entrance hole (area 1 cm^2) for the ion beam (Fig. 2.2.). The pumping speed S_p , necessary for reaching a vacuum of 7×10^{-8} Torr can now easily be calculated. The conductance of the diaphragm is about 10 l/s and the necessary pumping speed follows to be $S_p \approx 200 \text{ l/s}$. In the experimental arrangement used, an Ultec Boostivac pump has been installed. This pump is a sputter-ion pump combined with a sublimation pump.

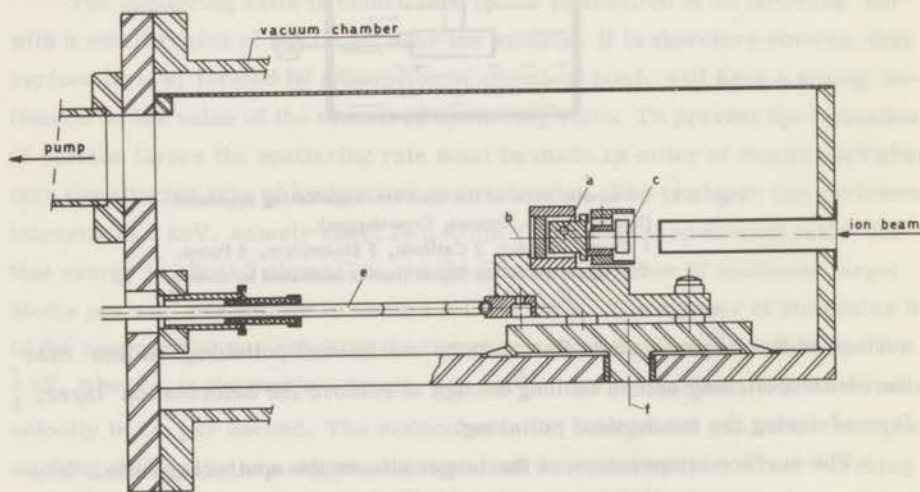


Fig. 2.2. The target holder as installed in the separate vacuum chamber. The crystal *c* can be turned, with the aid of the turning table around axis *f*. The rotation around *a* and *b* has been used to orientate the crystal in the holder.

The pumping speed for nitrogen, oxygen and water vapour is about 500 l/s, the pumping speed for noble gases is much lower, only a few litres per second. This was thought not to be disadvantageous because the noble gases do not easily form surface layers, as the sticking probability is low. Background pressures in the 10^{-8} range have been reached with this pump. During the bombardment of the target (with Ar^+ ions) the pressure in the separate vacuum chamber raised to about 1×10^{-5} Torr. This high argon pressure turned out to be disastrous for the sputter ion pump. The continuous bombardment of the electrodes by argon ions at these pressures reduces the lifetime of the electrode system and short-circuits are formed after a few days of pumping. The boostovac pump has therefore been replaced by a baffled Edwards oil diffusion pump with a pumping speed of 500 l/s. Pressures during the bombardment are now of the order of 8×10^{-7} Torr with a background pressure of 4×10^{-8} Torr. Concluding this section it can be said that the vacuum provisions are sufficient to reduce the formation of surface layers to an acceptable degree.

2.2.4. The target holder

In determining the sputtering ratio it is necessary to know the orientation of the used crystals with respect to the ion beam with an accuracy of at least 1° . To meet this requirement a special target holder for each crystal has been made (see Fig. 2.2). A (100)-crystal in the form of a flat cylinder (thickness 6 mm and diameter 16 mm) has been soldered on a triangular bar of copper. This bar can be pressed in the target holder. This target holder in turn has been mounted on a horizontal turning table with an angular range of 50° . For the measurements of the sputtering ratio as a function of the angle of incidence we want to rotate the crystals around a [011]-axis perpendicular to the [100]-direction. Therefore the [011]-axis had to be brought perpendicular to the horizontal turning table. This has been done by rotating firstly around axis a until the [011]-axis lies in a plane perpendicular to axis b. The tilting axis a is then fixed and the crystal can be turned around axis b till the [011]-axis is perpendicular to the turning table. The angle between zero position (along axis b) and the (100)-direction can be corrected for on the turning table. This rather complicated method is necessary because the front face of the (100)-crystals deviates a few degrees from the (100)-plane. The whole manipulations has been done with the aid of X-ray diffraction and has been performed at "Metaalinstituut T.N.O." in Delft. The error made in orientation of both [100]- and [011]-direction is less than 1° .

2.2.5. Determination of the sputtering ratio S

For the determination of S the method "weight loss of the target" has been chosen because we think this method to be still the most adequate way to measure absolute sputtering ratios. The weight loss as a result of the sputtering was chosen to be in the order of $1000 \mu\text{g}/\text{cm}^2$, corresponding with a depth of about 10^4 \AA . This is more than an order of magnitude higher than the mean penetration depth of the incoming projectiles, therefore the influence of projectile ions, remaining in the target, on the measured weight loss can be estimated to be smaller than 2 % for sputtering ratios higher than one.

For the weight measurements a microbalance with an accuracy of $5 \mu\text{g}$ has been used. Corrections have been applied for differences in barometric pressure and temperature if targets were used with a density different from the density of the balance weights.

The ion current onto the target has been measured with a current integrator, with an input voltage between 0 and -10 volts, depending on the beam current. The inaccuracy of the current integrator is smaller than 0.5 %. The secondary electron emission does not give rise to false current measurements because the electrons cannot escape the target holder. Electrons emitted from the target surface will describe helical orbits as a result of the magnetic field parallel to the surface and the dimensions are such that the electrons are always trapped in the holder (see thesis Rol, 1960, p. 34). The target is kept on a negative potential to prevent a disturbing current onto the target of electrons which are present in the ion beam for space charge compensation. With the expression mentioned in section 1.3 the value of the sputtering ratio follows directly from the weight loss and the total charge of the bombarding ions.

2.2.6. Accuracy of the measured sputtering ratio

The reproducibility of the measured sputtering ratio is determined by the error in the angle of incidence, the weight loss and the ion dose. It turns out that the spread of the measurements remains within 3 %, even for different crystals, if the targets are electropolished before each bombardment. This agrees fairly well with the estimations, made in the preceding sections. For targets bombarded previously the sputtering ratio was mostly found to be higher than the mean value of sputtering ratios measured on freshly electropolished crystals. This is demonstrated in Table I, where sputtering ratios are given together with

the removed weight during the measurement and the removed weight in an earlier measurement.

Table I

Sputtering ratios of a (100) Cu crystal under 20 keV Ar⁺ ion bombardment. Comparison between measurements on a freshly electropolished crystal and a crystal where a certain amount of material has already been removed in an earlier measurement.

Angle of incidence	earlier weight loss	sputtering ratio	weight loss during the measurement
18°	-	5.62	1.5 mg
	1.5 mg	5.67	1.5 mg
	7.7 mg	5.77	1.7 mg
30°	-	8.18	2.2 mg
	4 mg	8.35	2.1 mg
	6 mg	8.70	2.3 mg
3°	-	3.45	1.7 mg
	1.7 mg	3.52	1.8 mg

The error in the absolute value of the sputtering ratio is determined mostly by the angular spread of the ion beam, the induced radiation damage by the bombardment itself and the weight of the ions remaining in the target after the bombardment. In view of the considerations in the preceding sections and the results shown in Table I the error in the absolute value of the measured sputtering ratio can be estimated to be smaller than 3%. An exception is formed for the lead case, as shown in section 2.3.2.

2.3. EXPERIMENTAL RESULTS

2.3.1. The sputtering ratio as a function of the energy for normally incident ions

The sputtering yields for Ar⁺-ions on the (100), (110) and (111) planes of copper are shown in Fig. 2.3. Included for comparison are results of Southern et al. (1963), Magnuson et al. (1963), Snouse et al. (1965) and the polycrystalline results of Yonts et al. (1960). It can be seen that the agreement between the different authors is quite good, although the (110) results of Southern et al. seem

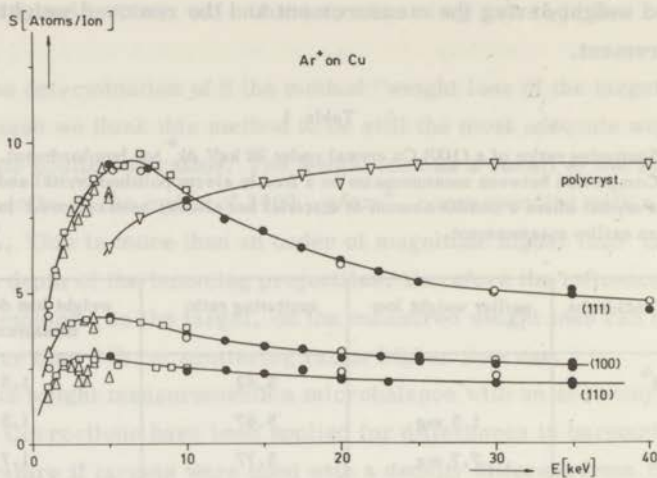


Fig. 2.3. The sputtering ratio as a function of the energy of normally incident Ar⁺ ions on different Cu crystals. The curves are drawn through the experimental points.

▽ Yonts et al. (1960), ◻ Magnuson et al. (1963),
 △ Southern et al. (1963), ○ Snouse et al. (1965), ● this work.

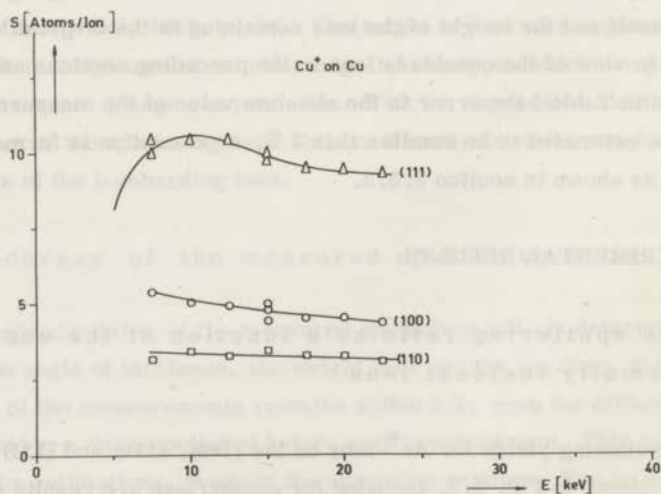


Fig. 2.4. The sputtering ratio as a function of the energy of normally incident Cu⁺ ions on different Cu monocrystals. The curves are drawn through the experimental points (this work).

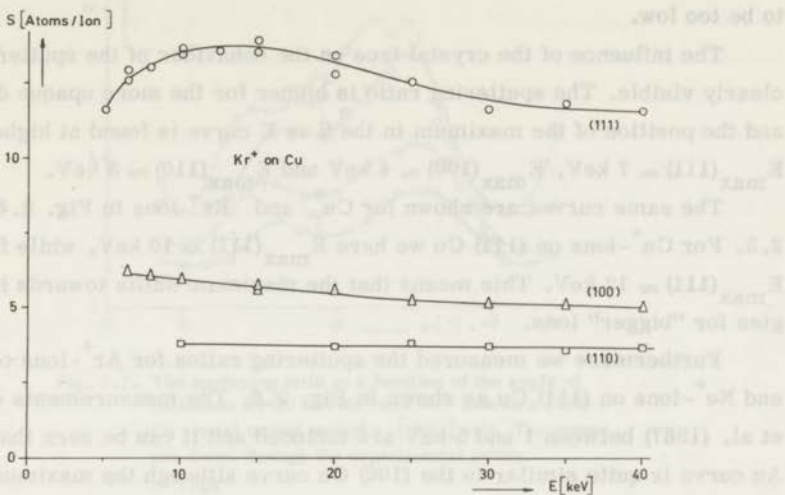


Fig. 2.5. The sputtering ratio as a function of the energy of normally incident Kr^+ ions. The curves are drawn through the experimental points (this work).

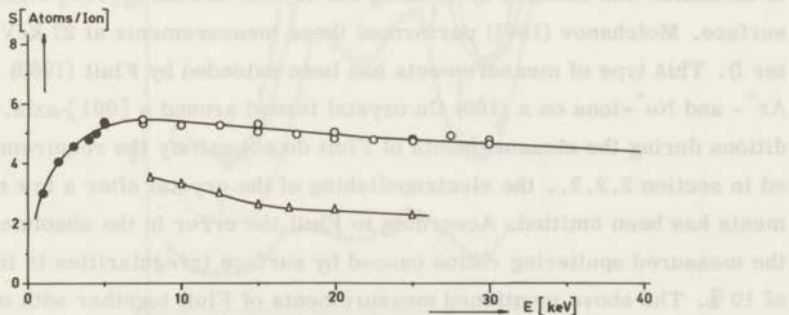


Fig. 2.6. The sputtering ratio as a function of the energy of normally incident ions. The curves are drawn through the experimental points.

- Ar^+ on (100) Au, Robinson et al. (1967).
- Ar^+ on (100) Au, this work.
- △ Ne^+ on (111) Cu, this work.

to be too low.

The influence of the crystal face on the behaviour of the sputtering ratio is clearly visible. The sputtering ratio is higher for the more opaque directions and the position of the maximum in the S vs E curve is found at higher energies: $E_{\max}^{(111)} \approx 7$ keV, $E_{\max}^{(100)} \approx 4$ keV and $E_{\max}^{(110)} \approx 3$ keV.

The same curves are shown for Cu^+ and Kr^+ ions in Fig. 2.4 and Fig. 2.5. For Cu^+ -ions on (111) Cu we have $E_{\max}^{(111)} \approx 10$ keV, while for Kr^+ -ions $E_{\max}^{(111)} \approx 12$ keV. This means that the maximum shifts towards higher energies for "bigger" ions.

Furthermore we measured the sputtering ratios for Ar^+ -ions on a (100) Au and Ne^+ -ions on (111) Cu as shown in Fig. 2.6. The measurements of Robinson et al. (1967) between 1 and 5 keV are included and it can be seen that the (100) Au curve is quite similar to the (100) Cu curve although the maximum seems to be located at a slightly higher energy (≈ 7 keV). In view of the low intensity of the Ne^+ -ion beam we were not able to measure below 8 keV and the maximum expected at an energy somewhere below 7 keV could not be located.

2.3.2. The sputtering ratio as a function of the angle of incidence

The first measurements of this kind have been performed in our laboratory by Rol et al. (1959), for a 20 keV Ar^+ -ion beam on a (100) Cu crystal; the angle of incidence was changed by rotating the crystal around a [011]-direction in the surface. Molchanov (1961) performed these measurements at 27 keV (see Chapter I). This type of measurements has been extended by Fluit (1963) for 20 keV Ar^+ - and Ne^+ -ions on a (100) Cu crystal turned around a [001]-axis. The conditions during the measurements of Fluit do not satisfy the requirement mentioned in section 2.2.2., the electropolishing of the crystal after a few measurements has been omitted. According to Fluit the error in the absolute values in the measured sputtering ratios caused by surface irregularities is in the order of 10%. The above mentioned measurements of Fluit together with our measurements are shown in Fig. 2.7. It can be seen that differences in the order of 25% occur. For the Ne^+ case we are able to demonstrate the experimental reason for the observed difference. We had difficulties with the reproduction of the measurement at 39° , above that the crystal exhibited a "milky spot" on the place where the ion beam hits the target. We found this "milky spot" only in the angular range 36° - 42° , the effect was very pronounced at 39° . To investigate the influence

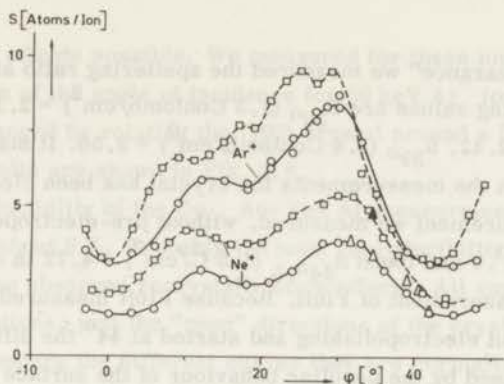


Fig. 2.7. The sputtering ratio as a function of the angle of incidence for 20 keV Ar^+ and Ne^+ ions on a (100) Cu crystal turned around a $[001]$ axis. The curves are drawn through the experimental points.

□ Fluit

○ this work

▲ △ later measurements around $\phi = 39^\circ$
(see section 2.3.2).

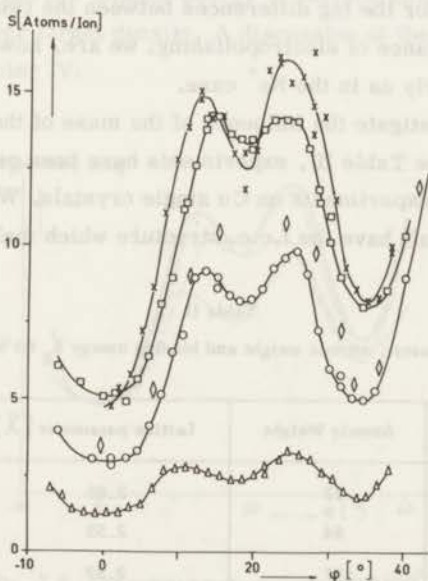


Fig. 2.8. The sputtering ratio for different (100) crystals bombarded with 20 keV Ar^+ ions, as a function of the angle of incidence. This angle has been changed by rotating the crystals around a $[011]$ axis in the surface. The curves are drawn through our experimental points. X Pb, □ Au, ◇ Cu (Rol et al. 1960), ○ Cu, △ Al.

of the "milky appearance" we measured the sputtering ratio at 39° for different doses, the resulting values are $S_{39^{\circ}}(1,3 \text{ Coulomb/cm}^2) = 2.17$, $S_{39^{\circ}}(1,6 \text{ Coulomb/cm}^2) = 2.42$, $S_{39^{\circ}}(2,4 \text{ Coulomb/cm}^2) = 2.56$. It may be said once more that between the measurements the crystal has been electropolished. After the last measurement we measured, without pre-electropolishing, the sputtering ratio at 34° and found $S_{34^{\circ}}(1,5 \text{ C/cm}^2) = 4.72$ in excellent agreement with the measurement of Fluit. Because Fluit measured his Ne^+ sputtering ratio curve without electropolishing and started at 44° the difference between the two curves is caused by the peculiar behaviour of the surface during the measurements around 39° . The target seems to be not too badly damaged however, because the general behaviour of the curve is not lost. We did test this furthermore by collecting the sputtered particles on a glass plate parallel to the bombarded surface and found, even at 39° Ne^+ bombardment of the target with "milky appearance", four [110] spots and one [100] spot on the glass plate. The nature of the "milky spot" on the target, although very interesting, has not been investigated.

An explanation for the big differences between the two Ar^+ curves must also be based on the omittance of electropolishing; we are, however, not able to demonstrate this as clearly as in the Ne^+ case.

In order to investigate the influence of the mass of the metal atoms and the lattice parameter (see Table II), experiments have been performed on Al, Au and Pb in addition to the experiments on Cu single crystals. We have chosen these metals because they all have the f.c.c. structure which makes a direct comparison

Table II
Lattice parameter, atomic weight and binding energy E_B for some metals

Metal	Atomic Weight	Lattice parameter [\AA]	E_B [eV]
^{13}Al	27	2.85	2.7
^{29}Cu	64	2.55	3.2
^{79}Au	197	2.87	3.7
^{82}Pb	207	3.49	1.9

of the directional effects possible. We measured for these metals the sputtering ratio as a function of the angle of incidence for 20 keV Ar^+ ions. The angle of incidence was changed by rotating the (100) crystal around a $[011]$ -axis in the surface. The results are shown in Fig. 2.8.

The reproducibility of the Cu-, Au- and Al-measurements is better than 3 %, for Pb it is about 8 %. Probably the poor reproducibility of the Pb measurements is due to the observed recrystallization effects. All curves show minima at the same directions, just the "open" directions of the crystal: $[100]$, $[411]$ and $[211]$. To compare the different curves they are normalized at 0° , as shown in Fig. 2.9. The Al curve has its first maximum at 11° , the Cu and Pb curve at 13° and the Au curve at 15° . For all curves one finds $S(35^\circ) = 1.5 S(0^\circ)$ within 15 %. It can be seen that the Al curve deviates from the others at the $[411]$ minimum at 19° and that the maxima are relatively lower with respect to the sputtering ratio at normal incidence. It can be seen that the form of the Cu and Pb curve is nearly identical, indicating that differences in lattice parameter and atomic mass compensate each other to a large extent. The equal absolute values of Au and Pb indicate that the low binding energy of surface atoms of Pb forms a compensation for its lower target density. A discussion of these experimental results will be given in Chapter IV.

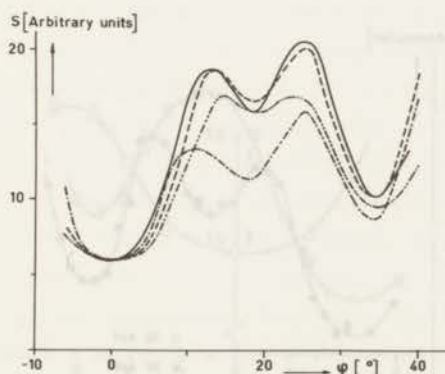


Fig. 2.9. The reduced sputtering ratio $S(\varphi)/S(0^\circ)$ as a function of the angle of incidence for 20 keV Ar^+ ion bombardment

— Pb
 - - - Cu
 - · - Al
 · · · Au

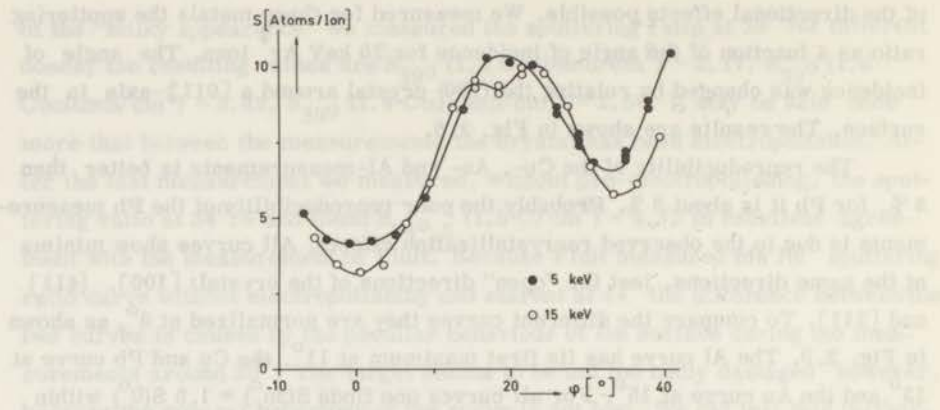


Fig. 2.10. The sputtering ratio as a function of the angle of incidence for 5 and 15 keV Ar^+ ions on a (100) Cu crystal, turned around a [011] axis in the surface. The curves are drawn through the experimental points (this work).

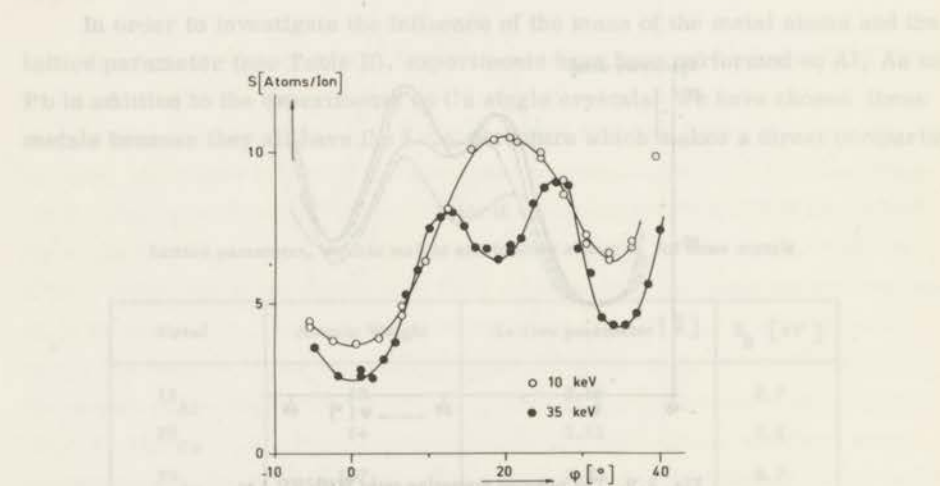


Fig. 2.11. The sputtering ratio as a function of the angle of incidence for 10 and 35 keV Ar^+ ions on a (100) Cu crystal, turned around a [011] axis in the surface. The curves are drawn through the experimental points (this work).

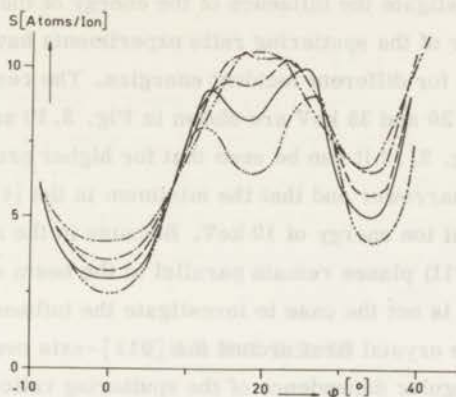


Fig. 2.12. The curves of figs. 2.8, 2.10 and 2.11, for Ar^+ ions on (100) Cu, turned around a $[01\bar{1}]$ axis.

- 5 keV
- 10 keV
- · - · - 15 keV
- 20 keV
- · — · — 35 keV

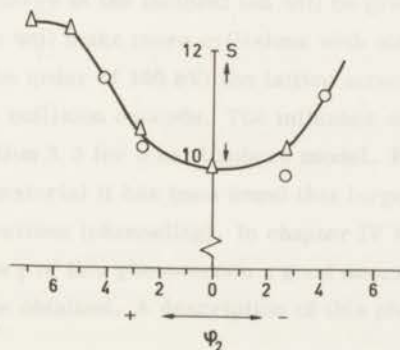


Fig. 2.13. The sputtering ratio as a function of the angle of incidence of a (100) Cu crystal turned around a $[01\bar{1}]$ axis, at $\varphi_1 = 25^\circ.5$. φ_1 is the angle in the preceding figures, changed by a rotation around a $[01\bar{1}]$ axis in the surface.

In order to investigate the influence of the energy of the incoming ions on the angular behaviour of the sputtering ratio experiments have been performed on a (100) Cu crystal for different incident energies. The results for Ar^+ -ion energy of 5, 10, 15, 20 and 35 keV are shown in Fig. 2.10 and 2.11. From the measurements in Fig. 2.12 it can be seen that for higher projectile energies the minima become narrower and that the minimum in the $[411]$ direction occurs only above an incident ion energy of 10 keV. Because in the above mentioned measurements the (011) planes remain parallel to the beam we did also a measurement where this is not the case to investigate the influence of that. We, therefore, turned the crystal first around the $[011]$ -axis over $25^\circ.5$ and after that measured the angular dependence of the sputtering ratio in turning round the $[01\bar{1}]$ -axis. We performed this measurement for 20 keV Ar^+ -ions on a (100) Cu crystal. The result is shown in Fig. 2.13. It can be seen that the maximum at $25^\circ.5$ is a minimum for the curve obtained by turning around the axis perpendicular on the first rotation axis. This means that in doing measurements of the sputtering ratio as a function of the angle of incidence a misorientation of a few degrees can lead to big errors.

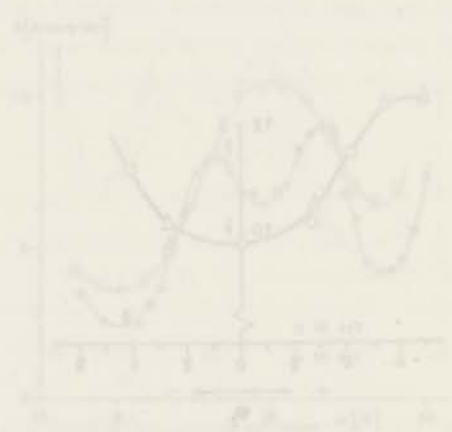


Fig. 2.11. The angular dependence of the sputtering ratio as a function of the angle of incidence for different incident ion energies of 5, 10, 15, 20 and 35 keV. The curves are shown for the $[011]$ and $[01\bar{1}]$ directions. The curves are shown for the $[011]$ direction. The curves are shown for the $[01\bar{1}]$ direction. The curves are shown for the $[011]$ direction.

CHAPTER III

THEORY OF COLLISIONS IN A METAL LATTICE

3.1. INTRODUCTION

The sputtering process is not yet completely understood, but the basic collision mechanisms, which are important for sputtering have been extensively studied in recent years. In our energy region (5-40 keV) the incident ion will lose most of the energy in successive elastic two body interactions and section 3.2 therefore deals with potentials which can be used for the calculation of deflection angles and energy transfers due to the interaction between atomic particles. Furthermore a short discussion concerning the classical approximation will be given. The energy of the incident ion will be given to a number of lattice atoms, which in turn will make more collisions with other lattice atoms. For lower energies (of the order of 100 eV) the lattice structure is known to be very important for such a collision cascade. The influence of the lattice structure is demonstrated in section 3.3 for a hard sphere model. From range measurements on monocrystalline material it has been found that large penetration tails occur in the open crystal directions (channeling). In chapter IV it is demonstrated that with the aid of a theory of this phenomenon a good description of the sputtering measurements can be obtained. A description of this phenomenon will be given in section 3.4.

3.2. THE INTERACTION POTENTIAL

The interaction potential between two free charges Z_1e and Z_2e is known to be the Coulomb potential

$$V(r) = \frac{Z_1 Z_2 e^2}{4\pi\epsilon_0 r} \quad (3.1)$$

where r is the distance between the charge centers. This potential can be used, for very high energies, for the interaction of two atomic particles. According to Bohr (1948) one could use the Coulomb potential for Ar^+ on Cu above an energy of $4 \cdot 10^5$ keV. For lower energies the nuclear charges are shielded by the orbital electrons. Bohr (1948) suggested an approximation in the form of an exponentially screened Coulomb (ESC) potential

$$V(r) = \frac{Z_1 Z_2 e^2}{4\pi\epsilon_0 r} \exp - \left[\frac{r}{a_b} \right] \quad (3.2)$$

where $a_b = K a_0 / (Z_1^{2/3} + Z_2^{2/3})^{1/2}$ and a_0 is the Bohr radius of the hydrogen atom; K is a constant of the order 1.

A more thorough treatment of the shielding of the nucleus by the electrons can be obtained with the aid of the Thomas-Fermi statistical method. The Thomas-Fermi atom is the result of the requirement that the total energy of the electrons is stationary with respect to variations in the electron density, subject to the subsidiary condition that the total charge remains constant. With the aid of some boundary conditions it is possible in this way to calculate the potential and the electron density distribution (Gombas 1949). Firsov (1958) performed a calculation for two atoms on a Thomas-Fermi model. The Firsov potential is

$$V(r) = \frac{Z_1 Z_2 e^2}{4\pi\epsilon_0 r} \bar{\phi} \left(\frac{r}{a_F} \right) \quad (3.3)$$

where $a_F = 0.8853 a_0 / (Z_1^{1/2} + Z_2^{1/2})^{2/3}$ and $\bar{\phi}$ is the Thomas-Fermi screening function.

In the postulates used to construct the Thomas-Fermi atom, it was explicitly assumed that the electron density distributions were completely independent. The exclusion principle dictates however that the occupancy of a particular state by one electron excludes it from occupancy by any others. The resulting exchange energy can be corrected for in the TF model leading to the so called Thomas-Fermi-Dirac (TFD) model. This calculation is performed by Abrahamson (1960) for two atoms using Firsov's method.

For lower energetic particles, in the order of 100 eV a Born-Maier potential

$$V(r) = A \exp - \left[r / a_{BM} \right] \quad (3.4)$$

is one that is suggested by quantummechanical calculations (1932). The constants A and a however are determined from thermodynamic properties of the particular crystal. Born-Maier constants for copper were deduced by Huntington (1953) from compressibility values; $A = 22.5 \text{ keV}$ and $a_{BM} = 0.196 \text{ \AA}$. Dependence of the values A and a_{BM} on the charge number Z are investigated by Anderson and Sigmund (1965).

A plot of the theoretical potentials is given in fig. 3.1. The unit of energy

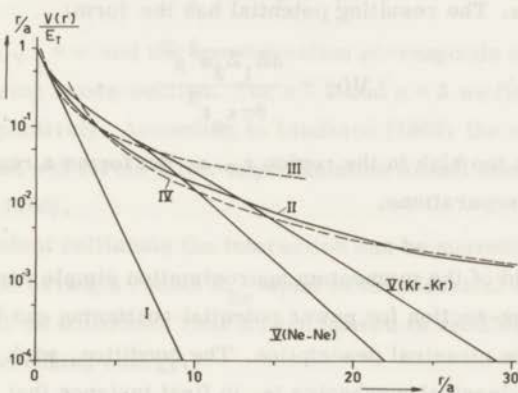


Fig. 3.1. Some two-atom potentials.

- I. E.S.C. potential (eq.3.2.)
- II. T.F. potential (eq.3.3.)
- III. Nielsen potential (eq.3.5.)
- IV. r^{-3} potential (eq.3.6.)
- V. T.F.D. potentials

appearing on the figure is defined by $E_T = Z_1 Z_2 e^2 / 4\pi\epsilon_0 a$, where $a = 0.8853 a_0 / (Z_1^{2/3} + Z_2^{2/3})^{1/2}$. The Bohr potential is the most widely used because of its simple mathematical form, but it falls off much too rapidly with distance for $r > a_0$. From range-energy relations it follows that probably the TF and TFD potentials are the most accurate. The advantage of the TF potential is that it is universal for all atoms when expressed in the appropriate parameters. A more

detailed description of the preceding subject can be found in an article by Abrahamson (1963).

Approximations to the above mentioned potentials are often chosen to be power potentials. Such potentials can be fitted to a more realistic potential in the region of interest and are chosen for mathematical convenience. An example is the r^{-2} potential (Nielsen, 1956) which is fitted to the ESC potential in the region near $r = a_b$. The Nielsen potential, with same value and first derivative at $r = a_b$ as the exponentially screened Coulomb potential is

$$V(r) = \frac{Z_1 Z_2 e^2 a_b \exp(-1)}{4\pi\epsilon_0 r^2} \quad (3.5)$$

Another example is the r^{-3} potential which can be fitted to a TF potential in the region $r = 4a$. The resulting potential has the form:

$$V(r) = \frac{3Z_1 Z_2 e^2 a^2}{8\pi\epsilon_0 r^3} \quad (3.6)$$

This potential is too high in the region $r \approx a$, but forms a reasonable approximation for larger separations.

With the aid of the momentum approximation simple expressions for the differential cross-section for power potential scattering can be obtained assuming the validity of the classical description. The condition, which must be satisfied for applicability of classical mechanics is, in first instance that $\lambda \ll a_s$, where a_s is a characteristic length for the scattering field and λ is the De Broglie wavelength divided by 2π . On the other hand the deflection angle ϑ must be larger than λ/a_s . For the length a_s one can take as a minimum for the used energies $a_s = a$ (about 0.1 \AA); λ is given by $\lambda = \frac{5 \cdot 10^{-2}}{\sqrt{ME}} \text{ \AA}$, where E is the relative energy in eV and M the mass of the incident particle in atomic units. Because we are not interested in energy transfers lower than the binding energy (a few eV) it can be seen that both conditions are fulfilled and classical mechanics may be used. We assume furthermore that the inelastic energy loss during a collision can be neglected for our purpose. In the momentum approximation the deflection is assumed to be small and the path nearly rectilinear. If $K_x(z)$ denotes the force perpendicular to the rectilinear path the deflection becomes

$$\vartheta = \int_{-\infty}^{+\infty} \frac{K_x(z) dz}{\mu v^2} \quad (3.7)$$

where $\mu = \frac{M_1 M_2}{M_1 + M_2}$ is the reduced mass of the relative motion of two particles

with mass M_1 and M_2 respectively. $K_x(z)$ is given by $\left(\frac{\partial V(\sqrt{z^2 + x^2})}{\partial x} \right)_{x=p}$

and for power potentials A/r^s the integration can

easily be performed. In elastic collisions the energy transfer T is given by

$T = T_m \sin^2 \vartheta/2$, where $T_m = 4M_1 M_2 / (M_1 + M_2)^2$. E and $E = \frac{1}{2} M_1 v^2$ (second particle initially at rest).

With the aid of these expressions we can find T as a function of the impact parameter p and we obtain

$$d\sigma = 2\pi p dp = \gamma_s \left(\frac{M_1}{M_2} \right)^{1/2} \frac{A^{2/s}}{E^{1/s} T^{1+1/s}} dT, \quad 1 < s < 4 \quad (3.8)$$

For $s = 1$ we have $\gamma_1 = \pi$ and the approximation corresponds exactly to the Rutherford scattering cross-section. For $s = 2$ and $s = 3$ we find $\gamma_2 = \pi^2/8$ and $\gamma_3 = 4^{1/3} \pi/3$ respectively. According to Lindhard (1963) the calculated cross-section for $s=2$ and $s=3$ forms a fair approximation for all energy transfers (see also Weysenfeld, 1966).

For more violent collisions the interaction can be approximated by scattering from a hard sphere having a radius R_{hs} equal to the classical distance of closest approach in a head-on collision. Thus a hard sphere is used with a radius which decreases with increasing energy.

3.3. FOCUSING COLLISIONS

It is commonly assumed that for sputtering in the keV region most of the sputtered particles are ejected from the surface as a result of a focusing collision chain. These focusing collision sequences are started by projectiles and by scattered particles through one or more non-focusing collisions. In the hard sphere approximation a simple demonstration of the focusing effect of a row of atoms is possible (Silsbee, 1957, Leibfried, 1959). This is illustrated in figure 3.2. If the angle ϑ_1 between the momentum vector of the first atom with the axis of the row of atoms is smaller than ϑ_F it is seen that we have $\vartheta_2 < \vartheta_1$, where ϑ_2 is the angle between the momentum vector of the second atom with the axis of the row of atoms. This means that the momentum vector is focused into the row of atoms. From the figure it follows that there is a finite probability for focusing as soon as the energy is so low that $D/2R < 1$. This means that for the direction where D is smallest the

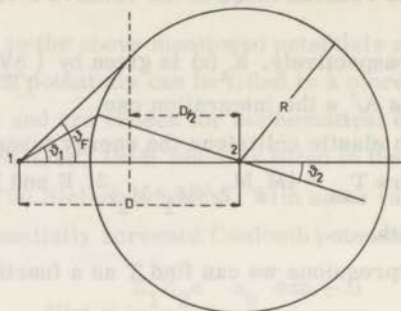


Fig. 3.2. Collision between two lattice atoms in a row, separation D . R is the hard sphere collision radius for an energy $E < E_F$. ϑ_F is the critical angle for focusing for this energy E .

focusing effect will be the most important. In f. c. c. crystals therefore focusing will predominantly occur along $\langle 110 \rangle$ -directions. Experimental evidence for the existence of focusing collision chains has been found in the preferential ejection of atoms sputtered from monocrystals and also in the energy distribution of atoms ejected in such a preferential ejection direction. The maximum energy E_F for which focusing can occur in a given direction is called "the focusing energy". It can be calculated from the relations $D/2R = 1$ and $E_F = 2V(R)$ if the potential is chosen. For a Born-Maier potential $V(r) = Ae^{-r/a}$ one finds $E_F = 2Ae^{-D/2a}$. This means for copper with $A = 22,5$ keV and $a = D/13$, $E_F = 60$ eV. The probability for an atom with energy E_0 to start in its first collision a focusing collision chain in a given $[110]$ -direction is $W_F(E_0) = \frac{1}{2} (1 - \cos \vartheta_F) = \frac{a}{2R} \ln \frac{E_F}{E_0}$ for $E_0 < E_F$. In calculating sputtering ratios some authors (Thompson, 1961,

Martynenko, 1965) calculate the number of recoils with energy $E_0 < E_F$ originating from an incident ion with energy E , assume this distribution to be isotropic and homogeneous and find from $W_F(E_0)$ the number of focusing collision chains in the direction of the surface. With the aid of loss mechanisms (Sanders et al., 1964, Nelson et al., 1962) the range of a focusing collision sequence can be calculated and the number of chains reaching the surface follows by an integration.

In these calculations an approximate expression for $W_F(E_0)$, namely $W_F(E_0) = \frac{a}{D} \ln \frac{E_F}{E_0}$ is taken, because it is thought that the chains with starting energy E_0

near E_F (this means $D \approx 2R$) are the most important. In view of calculations done by Sanders (1966) on recoil numbers in crystalline material, where it is found that the distribution of recoils in a non-correlated collision cascade is strongly peaked towards lower energy values, this assumption seems rather doubtful. A description of focusing without the use of a hard sphere approximation (Duesing et al., 1965) shows that the expressions for E_F and $W_F(E_0)$ are not very accurate. A further complication is the occurrence of other focusing mechanisms ("assisted focusing"). We will therefore not use a procedure as sketched above to describe our experimental results and not go into more details about focusing. A extensive treatment of focusing mechanisms can be found in the thesis of Weysenfeld (1966).

3.4. CHANNELING OF THE INCIDENT IONS

3.4.1. The concept of channeled particles was firstly introduced in range calculations by Robinson (1963). By channeling is meant that a particle path near the center of channel along a low index direction in a crystal may have a certain stability. The energy loss of a particle moving in that way will be low, leading to a long penetration length. This effect has been observed in range measurements by Davies (1961, 1962, 1963). Another demonstration of abnormal low stopping power is found in measurements of the energy loss of fast light ions passing through a thin foil (Nelson et al., 1963, Farmery et al., 1965, Lutz et al., 1966). Two distinct energy loss peaks were found demonstrating that once a particle is channeled it remains channeled. It follows from the remarks above that a channeled particle never comes close to a target atom reducing all those physical effects which require a close collision between incident particle and target atom. As an example for this we mention the work of Bøgh (1965) and Thompson (1965) about the directional dependency of nuclear reaction cross-sections in monocystals.

If an incident beam enters a mono-crystalline solid along a low index direction only part of it is channeled (governed motion). The other part of the beam experiences more or less hard collisions and the initial direction is lost after some time (ungoverned motion). This ungoverned motion is essentially unaffected by the structure of the substance and equivalent to motion in a random system. Particles moving along channels are subject to periodic forces, mainly focusing and occasionally defocusing. The transverse motion in a channel is roughly a long wave oscillation, combined with a short wave vibration with the

lattice period. If the energy of oscillation exceeds the barrier to a neighbouring channel a particle escapes from the channel. It follows from this, that an incident ion, with energy E and angle ψ with the channel axis, entering the crystal, close to the channel axis, remains in the channel if $E \sin^2 \psi$ is smaller than the barrier energy. These cursory considerations indicate that for higher particle energies the critical angle becomes smaller than for low-energetic particles. On the other hand the criterion of entering the solid close to the channel axis is less important for higher-energetic particles. This means that the channeled fraction of a beam entering a crystal along a channel axis becomes larger for higher energies. In the theory of Lindhard (1965) about the influence of crystal lattice on motion of energetic charged particles the above mentioned kind of channeling (remaining in a channel) is called "proper channeling". In Lindhard's picture there is also place for "improper channeling"; in this case the particle interacts with strings of atoms, it has no close collisions and moves from one channel to another. In the next section we will give a derivation of formulae important for us following closely the treatment of Lindhard (1965). Other theoretical treatments of channeling are given by Lehmann and Leibfried (1963), Erginsoy (1964, 1965) and Nelson et al. (1963). As mentioned before computer studies were performed by Robinson and Oen. Other computer studies are done by Lutz et al. (1964). The theory of Lindhard however, is the most general and adequate to our purpose.

3.4.2. Theory of Lindhard

In order to find an approximative procedure for the directional effects Lindhard introduces four assumptions:

a. The angles of scattering are small. If the angle of scattering in the laboratory system, φ , and in the center of mass system, ϑ , are small, we have

$$\varphi \approx \frac{M_2}{M_1 + M_2} \vartheta, \text{ where } M_1 \text{ and } M_2 \text{ are the masses of the incident particle and target atom respectively.}$$

b. String assumption. If a particle moves at a small angle with a row of atoms (string) the successive collisions with atoms in the string are not independent. A description of the particle path is supposed to be possible with a string potential, where the string is characterized by the constant distance d of the atoms placed on a straight line.

c. Classical description. According to Lindhard the classical description of

many successive collisions with atoms in a string remains valid.

d. The assumption of a perfect lattice without vibrations.

The basis of the theory is that the motion of a particle is influenced by many consecutive atoms if certain conditions are fulfilled. This leads to a transverse continuum potential of a string of atoms. This potential $U(r)$, can be defined as an average potential in the following way

$$U(r) = \int_{-\infty}^{\infty} \frac{dz}{d} V(\sqrt{z^2 + r^2}) \quad (3.9)$$

where V is the ion-atom potential, r the distance from the string and z a direction parallel to the string.

For $r \gg a$ the string potential becomes

$$U(r) \approx \frac{3Z_1 Z_2 e^2 a^2}{4\pi \epsilon_0 d r^2} \quad (3.10)$$

the corresponding ion-atom potential is $V(r) = 3/2 Z_1 Z_2 e^2 a^2 / 4\pi \epsilon_0 r^3$, fitting reasonably well to a TF potential for $r \gtrsim 4a$.

For higher energies where the important region for the string potential is thought to be in the region $r \approx a$ the stringpotential reads:

$$U(r) = \frac{\pi Z_1 Z_2 e^2 a}{8\pi \epsilon_0 d r} \quad (3.11)$$

The low energy expression should be used at energies below

$E^1 = 2Z_1 Z_2 e^2 d / 4\pi \epsilon_0 a^2$. For the ion target combinations we investigate the value of E^1 lies in the order of 1 MeV, we will therefore confine the discussion to the low energy case.

A qualitative condition for the continuum approximation is obtained if we demand that the scattering in the vicinity of the distance of closest approach is due to many atoms. If a particle moves at an angle ψ in the middle of the channel (far from the string) with a velocity v the collision time Δt is of the order $r_{\min} / v \sin \psi$ and the condition can be put in the form

$$\Delta t \cdot v \cos \psi \approx \frac{r_{\min}}{\psi} > d \quad (3.12)$$

The distance of closest approach is determined by

$$U(r_{\min}) = \frac{1}{2} M_1 v^2 \sin^2 \psi \quad (3.13)$$

From 3.12 and 3.13 we find for the critical angle ψ_2

$$\psi_2 = (3 Z_1 Z_2 e^2 a^2 / 4 \pi \epsilon_0 d^3 E)^{1/4} \quad (3.14)$$

For an incident beam of particles parallel with the string direction we now can find the minimum distance to the center of the string which a particle is allowed to have, in order to apply the continuum description. The deflection angle φ in the laboratory system for the used ion-atom potential (3.6) is

$\varphi = 3 Z_1 Z_2 e^2 a^2 / 4 \pi \epsilon_0 E p^3 = \psi_2^4 d^3 / p^3$, where p is the impact parameter of the incident ion. The condition $\varphi < \psi_2$ gives us the minimum distance $p_{\min}(o)$:

$$p_{\min}(o) = \psi_2 d \quad (3.15)$$

So we simply have $p_{\min}(o) = r_{\min}$. This means that for an incident particle the transverse energy with respect to the string is equal to $U(p)$ where p is the impact parameter as should be expected for a rigid potential wall. It follows from this that a particle leaves the string at the same angle as it had prior to the collision and loses no energy to the string.

The fraction of the incident beam, parallel to a string, that enters the random beam can be given by $\frac{\pi p_{\min}^2(o)}{2 \pi p_o^2}$, where $\pi p_o^2 = (Nd)^{-1}$, with N the number density of the target and d the stringparameter. For the used potential we get

$$\frac{\pi p_{\min}^2(o)}{2 \pi p_o^2} = \pi N d^{3/2} \left(\frac{3 a^2 Z_1 Z_2 e^2}{4 \pi \epsilon_0 E} \right)^{1/2} \quad (3.16)$$

It can be seen that the non-channeled fraction of the beam becomes unity for a critical energy E_c , given by

$$E_c^{1/2} = \pi N d^{3/2} \left(\frac{3 a^2 Z_1 Z_2 e^2}{4 \pi \epsilon_0} \right)^{1/2} \quad (3.17)$$

For a beam entering the solid with an angle Ψ to the string direction it is more difficult to calculate the fraction that enters the random beam. According to Lindhard the fraction of channeled particles becomes zero for an angle $C\Psi_2$, where C is a constant of the order one. With the condition $fE\Psi^2 + U(p_{\min}(\Psi)) = E\Psi_2^2$, where f is some number between zero and one we find as a rough approximation for the fraction entering the random beam:

$$\frac{\pi p_{\min}^2(\Psi)}{\pi p_0^2} = \left[\frac{p_0^2}{p_{\min}^2(o)} + \left(1 - \frac{p_0^2}{p_{\min}^2(o)}\right) \frac{\Psi^2}{(C\Psi_2)^2} \right]^{-1}, \text{ for } \Psi < C\Psi_2 \quad (3, 18)$$

We have seen that a beam of particles incident on a monocrystalline target can be divided roughly in two parts, the random beam and the aligned beam. The aligned beam is characterized by an abnormal low energy loss. One can ask if particles in the aligned beam can enter the random beam and vice versa. In a perfect lattice such transitions have a very low probability. An ion in the aligned beam will in the continuum approximation keep a constant energy perpendicular to the strings, changing merely its azimuthal angle in a more or less random manner. It remains therefore in the aligned beam. An ion in the random beam will need a comparatively close collision to get into the channel; such close collisions are not allowed in the continuum description. Scattering from the random beam to the aligned beam therefore seems prohibited.

Deviations from this idealized picture arise for instance from thermal vibrations, defects and impurities in the lattice. For a discussing of these phenomena and a more exact description of the string effect we refer to the work of Lindhard (1965).

CHAPTER IV

THEORY OF SPUTTERING AND COMPARISON WITH EXPERIMENTAL RESULTS

4.1. INTRODUCTION

A qualitative explanation of sputtering results measured as a function of the angle of incidence on monocrystals has been given by Fluit (1963). He assumes that the sputtering ratio is determined by the "transparency" of the crystal in the direction of the incident beam, where a high transparency means that the mean penetration depth of the incident ions is high and thus the sputtering ratio is low. This is in fact based on the theory of Rol (1960), where it is assumed that the sputtering ratio is proportional to the mean transferred energy of the incident ions to the target atoms in the first collision and inversely proportional to the mean free path of the incident ions. Fluit defined the transparency as the inverse of the collision probability in the first ten layers. A quantitative approach based on a transparency model has been given by Southern et al. (1963), Magnuson et al. (1963), and Odintsov et al. (1963). In section 4.2 we will summarize two of these transparency theories together with their applications. The theory of Odintsov can be used directly for our angular measurements and in section 4.2.3 we will give a description of our results with this theory. A discussion of the hazy behaviour of the proportionality constants in the Odintsov theory will be given. In the next section an investigation of the influence of the channeling phenomenon on single crystal sputtering leads to an extension of the transparency model. It is shown that a description of our results can be obtained based on the idea that a channeled particle does not contribute to sputtering.

4.2. TRANSPARENCY THEORIES

4.2.1. Theory of Southern, Willis and Robinson (1963).

The basic assumptions of the theory are that the sputtering yield is determined with sufficient accuracy by the first collision of the incident ion with an atom of the target and that the collision may be imagined to take place between hard spheres whose size determines the total cross section for scattering of the incident ions by the target atoms. The yield is regarded as proportional to the stopping power of the target for incident ions at their initial energy, i. e., as proportional to the average energy transferred to a target atom in a collision and as inversely proportional to the mean free path of the incident ions to their first collisions. Thus, according to Southern et al., the sputtering yield for ions of energy E , normally incident upon a target surface with orientation (hkl) may be written as

$$S_{hkl}(E) = \alpha \tau_{hkl}(E) E / \lambda_{hkl}(E) \quad (4.1)$$

where α is a proportionality constant, $\lambda_{hkl}(E)$ the mean free path of the incident ion, and

$$\tau_{hkl}(E) = 2 T_{hkl}(E) / T_m(E) \quad (4.2)$$

where $T_{hkl}(E)$ is the average energy transferred to a target atom in the first collision of the incident ion and $T_m(E)$ the maximum energy that can be transferred in a single collision. So far this theory is exactly the same as the theory of Rol for polycrystalline targets. The extension lies in the definition of a mean free path in monocrystals, as is done in a way described below. The target is considered to be an array of spheres arranged on a crystalline lattice. For ions which are incident upon the surface of the crystal in a $[hkl]$ direction an "elementary crystal" is considered defined by the elementary translations t_{hkl} , $t_{h'k'l'}$, $t_{h''k''l''}$, where for cubic lattices it may be remarked that $[h'k'l']$ and $[h''k''l'']$ are perpendicular to $[hkl]$ and to each other. This elementary crystal is thought to be uniformly irradiated with ions, a fraction p_{hkl} of them will make collisions within the element, while the balance will pass through it without making collisions at all. It is from this property of the model that the term "transparency" arises. The average distance from the surface which the colliding ions move in reaching their collision points x_{hkl} is their contribution to the first mean free path of all the ions. The authors now assume that ions which

do not make collisions in the elementary crystal have a mean free path λ_0 , which is independent of their direction. The mean free path for all ions may than be written as

$$\lambda_{hkl}(E) = p_{hkl} x_{hkl} + (1 - p_{hkl}) \lambda_0(E) \quad (4.3)$$

The above way of defining a mean free path for all ions demonstrates the fundamental difficulty of the extension of Rol's polycrystalline theory to the monocrystalline case (in the hard sphere approximation). It is easily seen that in a hard sphere model the free path of an ion will be infinite if it moves along an open direction of the crystal. Taking this into account would make equation (3) useless. This problem can not be solved by taking a mean value over the inverse free path because there are always particles having their first collision just at the surface leading to a first free path equal to zero. As seen above the authors solve the problem rather artificially by assuming a uniform mean free path $\lambda_0(E)$ which will be used as a fitting parameter. The energy transferred in a collision may be defined in terms of the impact parameter b . For hard sphere interactions,

$$\tau(E) = 2 [1 - \langle b^2/R^2 \rangle_{hkl}], \quad (4.4)$$

where $\langle \rangle$ denotes the average value and R the collision radius. If the spheres do not overlap $\langle b^2/R^2 \rangle = \frac{1}{2}$ and $\tau(E) = 1$, but for large enough spheres this will not be true because of shadowing. It is assumed that shadowing may be ignored for those ions which make collisions beyond the elementary crystal. Then

$$\tau(E) = 1 + p_{hkl} [1 - 2 \langle b^2/R^2 \rangle_{hkl}] \quad (4.5)$$

Finally, introducing (3) and (5) into (1) the authors obtain an expression for the sputtering ratio:

$$S_{hkl}(E) = \alpha [1 + p_{hkl} (1 - 2 \langle b^2/R^2 \rangle_{hkl})] E / [p_{hkl} x_{hkl} + (1 - p_{hkl}) \lambda_0(E)] \quad (4.6)$$

Equation (6) was fitted to the experimental data (sputtering ratios for Ar^+ ions normally incident on different Cu monocrystals in the energy range 1 - 5 keV) by evaluating p_{hkl} , x_{hkl} and $\langle b^2/R^2 \rangle_{hkl}$ for a particular hard sphere radius using a computer program. The values of α and λ_0 were then obtained from the data by the method of least squares. This procedure was repeated for each of several values of the radius. A value for the hard sphere was selected from the minimum deviation between theory and experiment. The result of such a fitting is given in fig. 4.1 for 5 keV Ar^+ ions normally incident on different monocrystals. The parameters derived from the fitting for different energies are given in table I.

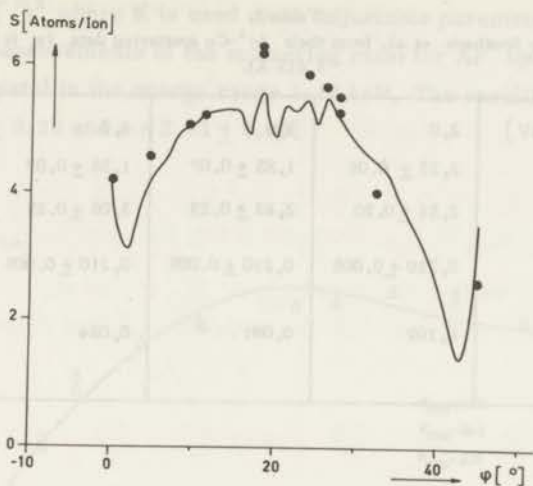


Fig. 4.1. The sputtering yields of (0kl) Cu crystals under normally incident 5-keV Ar⁺ ion bombardment, plotted against the angle between the surface normal and the [001] direction, the line represents the theoretical yield, the points the experimental. (Southern et al.)

The results of the data fitting are very gratifying in that the calculated and observed yield are always in quite good agreement. Contrarily to the authors opinion we think that the occurrence of the two deep minima not precisely at [001] and [011] is due to the assumption of the uniform mean free path $\lambda_0(E)$. From table I it follows that the parameter α instead of being independent of energy decreases with increasing energy and in fact is proportional to $E^{-1/2}$. The value of R on the other hand is apparently independent of energy instead of decreasing with increasing energy as was anticipated. Finally the hard core radius is substantially larger than expected from the hard sphere approximation of the E.S.C. potential, as is shown by the values of R_{Bohr}/a_0 entered in the table.

In spite of the fact that the theory gives a good description of the results the applicability of the model is rather limited. It can be seen that the extension of the mean free path theory of RoI for polycrystalline materials towards monocrystalline targets is not possible without serious difficulties.

Table I.
Parameters derived by Southern et al. from their Ar⁺-Cu sputtering data. (a_0 is the unit cell edge 3,615 Å).

Ar ⁺ ion energy [keV]	2,0	3,0	4,0	5,0
α/a_0 [keV ⁻¹]	2,25 ± 0,08	1,85 ± 0,07	1,56 ± 0,07	1,35 ± 0,05
λ_0/a_0	2,51 ± 0,20	2,82 ± 0,23	3,06 ± 0,25	3,18 ± 0,25
R/a_0	0,210 ± 0,005	0,210 ± 0,005	0,210 ± 0,005	0,210 ± 0,005
R_{Bohr}/a_0	0,102	0,091	0,084	0,080

4.2.2. Theory of Magnuson and Carlston (1963).

In this theory it is again supposed that the process is determined sufficiently accurately by the first collision. Contrarily to the assumption in the preceding theory it is assumed that those ions that pass through the first repeat distance of the crystal without making a collision are assumed to penetrate deeply enough, so that their contribution to the sputtering yield is negligible. The sputtering yield is assumed to be proportional to the product of the absolute value of the momentum transferred to a lattice atom in the first collision and the probability that a collision occurs between the incident ion and a lattice atom, no matter at what depth this first collision occurs. The collision probability is expressed as an opacity, i. e. the ratio of closed to total area in a representative area of the lattice. The sputtering ratio can then be written as

$$S_{hkl}(E) = K_{hkl} E^{\frac{1}{2}} P_{hkl}(E) \quad (4.8)$$

where K_{hkl} is a proportionality constant which depends on the crystal plane bombarded, E the energy of the incident ion, $P_{hkl}(E)$ the probability of a collision between an ion and a lattice atom, for an ion incident normally on a (hkl) plane. The lattice is considered to consist of hard spheres located at normal lattice positions of a f. c. c. lattice. The radius used in the calculations was taken as $R = cR_{Bohr}$, where c is a constant and R_{Bohr} the hard core approximation to the ESC potential. The Bohr screening constant a_b is supposed to be given by $a_b =$

$Ka_0 / (Z_1^{2/3} + Z_2^{2/3})^{1/2}$ where K is used as an adjustable parameter. The model has been fitted to measurements of the sputtering ratio for Ar^+ ions on a (100), (110) and (111) Cu crystal in the energy range 1–10 keV. The resulting K and c values were $K = 1.20 \pm 0.20$ and $c = 2.35 \pm 0.05$.

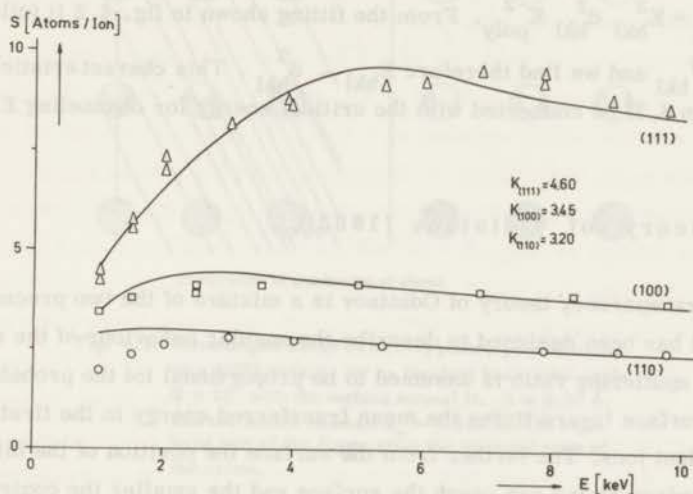


Fig. 4.2. The sputtering ratio as a function of the energy for normally incident Ar^+ ions on different Cu crystals. The curves are theoretical, the points experimental. (Magnuson et al.) The units of K_{hkl} are $(keV)^2$.

The agreement with the data is fairly good. (See fig. 4.2). It is interesting to compare formula (8) with an expression for the sputtering ratio of polycrystalline targets (Rol 1960). Rol's formula for normal incidence can be written as

$$S_{poly}(E) = K_{poly} E N \pi R^2 \quad (4.9)$$

where E the energy of the incident ions, N the number density of the target atoms, R the hard sphere collision radius and K_{poly} a proportionality constant. Equation (8) can be rewritten, for a low-index crystal face, as

$$S_{hkl}(E) = K_{hkl} E^{1/2} N \pi R^2 d_{hkl} \quad (4.10)$$

where $(N d_{hkl})^{-1}$ is the area "belonging" to one atom in the surface.

Comparison of equations (9) and (10) shows that the difference between both expressions is formed by a $S \sim E^{1/2}$ relation for the monocrystalline case and a

$S \sim E$ relation for the polycrystalline case. It follows from both formulae that we have for normal incidence:

$$S_{\text{hkl}}(E) = (E_{\text{hkl}})^{\frac{1}{2}} E^{-\frac{1}{2}} S_{\text{poly}}(E) \quad (4.11)$$

where $E_{\text{hkl}} = K_{\text{hkl}}^2 d_{\text{hkl}}^2 K_{\text{poly}}^{-2}$. From the fitting shown in fig. 4.2 it follows that $K_{\text{hkl}} \sim d_{\text{hkl}}^{\frac{1}{2}}$ and we find therefore $E_{\text{hkl}} \sim d_{\text{hkl}}^3$. This characteristic energy will (section 4.3) be connected with the critical energy for channeling E_c (see 3.17).

4.2.3. Theory of Odintsov (1963).

The transparency theory of Odintsov is a mixture of the two preceding models and has been designed to describe the angular behaviour of the sputtering ratio. The sputtering ratio is assumed to be proportional to the probability of a hit in the surface layers times the mean transferred energy in the first collision of the incident ions. The further from the surface the position of the hit atom, the fewer secondary atoms can reach the surface and the smaller the contribution of this collision to the sputtering yield. Furthermore sputtering increases when the incident particles are at an angle, because in this case not only the secondary, but also the hit atoms can acquire an appreciable velocity normal to the surface. Thus the coefficient of proportionality between sputtering and the energy transferred to an atom should depend on the position of the hit atom and the angle of incidence of the beam particles on the target. If $\bar{E}_i(\varphi)$ is the mean transferred energy to an atom in layer i (i counted from the surface) and $A_i(\varphi)$ the visible surface of that atom the sputtering ratio may be written as:

$$S(\bar{E}, \varphi) = \sum_i \alpha_i(\varphi) A_i(\varphi) \bar{E}_i(\varphi) / A_0 \cos \varphi \quad (4.12)$$

where A_0 is the area belonging to one atom, φ the angle of incidence with respect to the surface normal and $\alpha_i(\varphi)$ a proportionality constant depending on the angle φ and the layer number i , where i is counted from the surface. The average energy transferred to an atom in the case where part of it is hidden by an atom above is given by the following formula, derived in the hard sphere approximation:

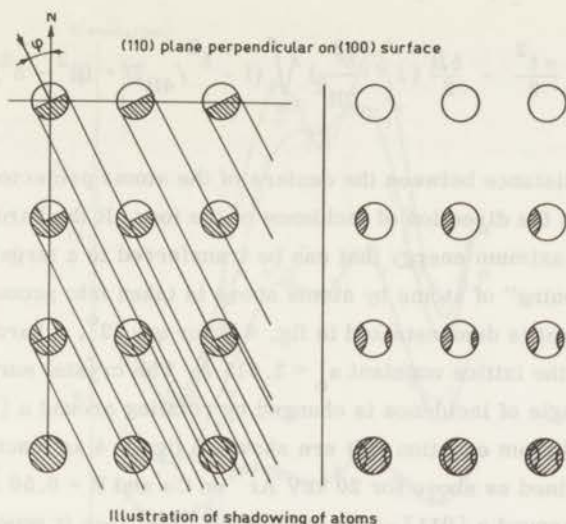


Fig. 4.3. Screening of atoms in a (110) plane, perpendicular on a (100) surface, for an incident beam with angle $\varphi = 22^\circ$ with the surface normal N . $R = 0.50 \text{ \AA}$ and the lattice constant $a_0 = 3.615 \text{ \AA}$. The right hand part of the figure gives the screened parts of the atoms.

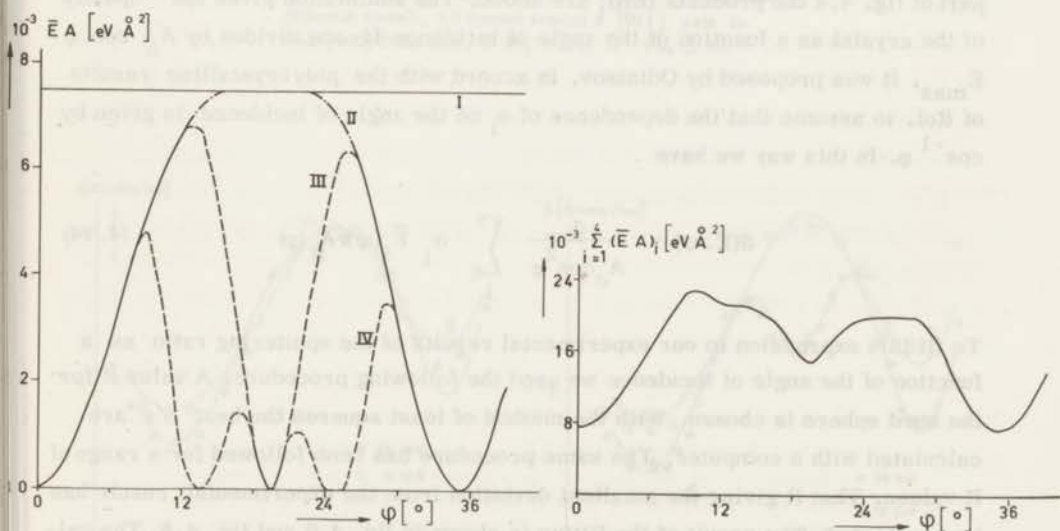


Fig. 4.4. (a) The transferred energy times the visible area for 20 keV Ar ions onto the different Cu atom layers as a function of the angle of incidence.

(b) The "opacity" of the crystal as a function of the angle of incidence, changed by rotating the crystal around a [011] axis in the (100) front face. $R = 0.50 \text{ \AA}$ and $a_0 = 3.615 \text{ \AA}$.

$$\bar{E}_i A_i = E_{\max} \left[\frac{\pi \delta^2}{2} - \frac{\delta R}{2} \left(1 + \frac{\delta^2}{2R^2} \right) \sqrt{\left(1 - \frac{\delta^2}{4R^2} \right) + (R^2 - \delta^2)} \arcsin \frac{\delta}{2R} \right] \quad (13)$$

where δ is the distance between the centers of the atoms projected on a plane perpendicular to the direction of incidence of the ions, R the hard sphere radius and E_{\max} the maximum energy that can be transferred to a target atom. In this way the "screening" of atoms by atoms above is taken into account. This "screening" effect is demonstrated in fig. 4.3 for $\varphi = 22^\circ$, a hard sphere radius $R = 0.50 \text{ \AA}$ and the lattice constant $a_0 = 3.615 \text{ \AA}$. The crystal surface is a (100) plane and the angle of incidence is changed by rotating around a [011]-axis. The results obtained from equation (10) are shown in fig. 4.4 as function of the angle of incidence defined as above for 20 keV Ar^+ on Cu and $R = 0.50 \text{ \AA}$. In turning a f. c. c. crystal around a [011]-axis in the (100) front face it appears that the even layers are never shadowed by odd layers, therefore layer 1 and 2 are taken together as I, 3 and 4 as II etc. The first two layers are always visible, this means that $(\bar{E}A)_I$ is simply given by $\frac{1}{2} \pi R^2 E_{\max}$ as shown in the figure. The deeper layers show maxima and minima as a result of the screening. In the right part of fig. 4.4 the products $(\bar{E}A)_i$ are added. The summation gives the "opacity" of the crystal as a function of the angle of incidence if one divides by $A_0 \cos \varphi E_{\max}$. It was proposed by Odintsov, in accord with the polycrystalline results of Rol, to assume that the dependence of α_i on the angle of incidence is given by $\cos^{-1} \varphi$. In this way we have

$$S(E, \varphi) = \frac{1}{A_0 \cos^2 \varphi} \sum_i \alpha_i \bar{E}_i(\varphi) A_i(\varphi) \quad (4.14)$$

To fit this expression to our experimental results of the sputtering ratio as a function of the angle of incidence we used the following procedure. A value R for the hard sphere is chosen. With the method of least squares the best α 's are calculated with a computer. The same procedure has been followed for a range of R values. That R giving the smallest deviation from the experimental result has been selected. The result of the fitting is shown in fig. 4.5 and fig. 4.6. The values for R and α are given in table II.

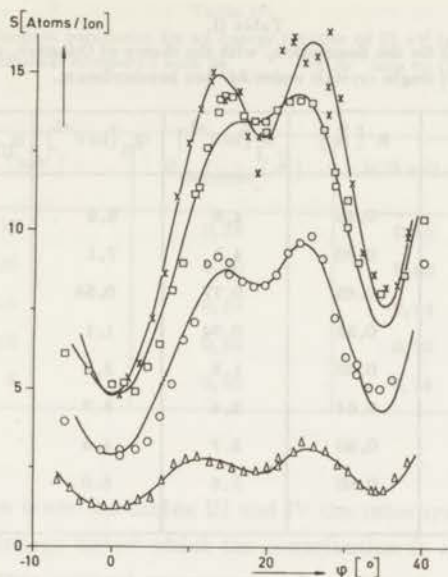


Fig. 4.5. Comparison of Odintsov's theory with our experimental results. The curves are theoretical, the used values for the fitting parameters are given in Table II. The points are experimental for 20 keV Ar ions onto different metals, all turned around a $[011]$ axis in their (100) front face. X Pb, \square Au, \circ Cu, Δ Al.

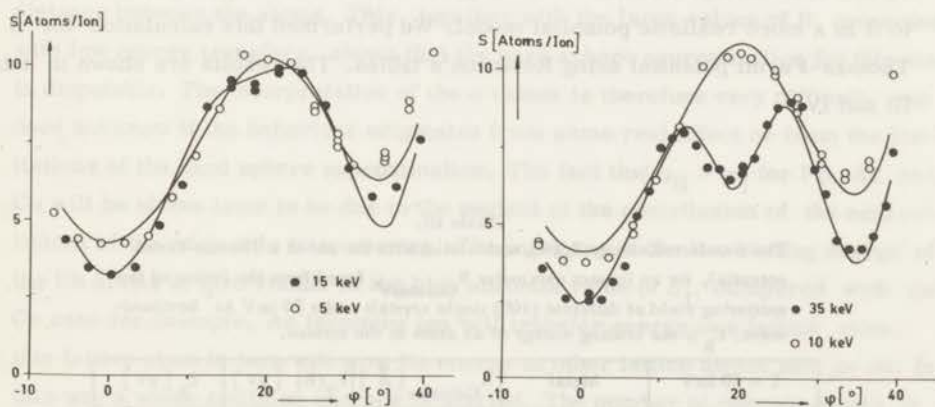


Fig. 4.6. Comparison of Odintsov's theory with our experimental results for 5-, 10-, 15- and 35 keV Ar ions on (100) Cu turned around a $[011]$ -axis. The curves are theoretical, the used values for the fitting parameters are given in Table II.

Table II.

The fitting parameters used for the description, with the theory of Odintsov, of the angular dependent sputtering of different (100) single crystals under Ar^+ ion bombardment.

E [keV]	Metal	R [\AA]	α_I [keV^{-1}]	α_{II} [keV^{-1}]	α_{III} [keV^{-1}]	α_{IV} [keV^{-1}]
20	Pb	0.85	4,8	6.6	6.1	-
20	Au	0.70	4,5	7.1	2.2	-
20	Al	0.65	0.77	0.58	0.57	0.41
35	Cu	0.58	0.94	1.1	1.3	0.01
20	"	0.60	1.8	2.7	1.3	-
15	"	0.64	2.4	3.9	1.0	-
10	"	0.80	2.7	4.6	-	-
5	"	0.80	5.8	8.0	-	-

DISCUSSION

The hard sphere radius R has a two fold meaning in this description. It determines the cross-section for a collision important for sputtering, at the other hand it determines the screening of deeper laying atoms. In the hard sphere model the two "sizes" coincide, but the value of R is of course larger than the distance of closest approach in a head-on collision. To get an idea about the meaning of the values of R one can calculate the energy transfer for an impact parameter equal to R in a more realistic potential model. We performed this calculation for a Thomas-Fermi potential using Robinson's tables. The results are shown in table III and IV.

Table III.

The transferred energy $E_T(R)$, calculated with the aid of a Thomas-Fermi potential, for an impact parameter R_{Odintsov} , found from the fitting of the sputtering yield of different (100) single crystals under 20 keV Ar^+ bombardment. E_B is the binding energy of an atom at the surface.

E = 20 keV	Metal	R_{Odintsov} [\AA]	$E_T(R)$ [eV]	E_B [eV]
	Pb	0,85	20	1,9
	Al	0,65	35	2,7
	Au	0,70	50	3,7
	Cu	0,60	75	3,2

Table IV.

The impact parameter for an energy transfer of 75 eV in the TF potential compared with R_{Odintsov} for Ar^+ ions on (100) Cu.

E [keV]	R_{Odintsov} [\AA]	b(75 eV) [\AA]
35	0,58	0,58
20	0,60	0,60
15	0,64	0,64
10	0,80	0,70
5	0,80	0,78

As can be seen from the tables III and IV the interpretation of R as an impact for a certain energy below which the contribution to sputtering can be neglected is not bad. This critical energy must depend on the binding energy E_B and on the other hand on the size of energy losses during transport of momentum towards the surface. The influence of the binding energy is visible for the Pb case where we have the lowest binding energy (1.9 eV) of the surface atoms and also the lowest critical energy (20 eV). We think however that the usefulness of the found energy values is limited because the used R values are a kind of mean value of maximum impactparameter important for sputtering and screening radius. This screening radius is, for a non hard sphere model a function of the distance between the atoms. This, together with the large values of R, connected with low energy transfers, shows that the hard sphere approximation for this case is disputable. The interpretation of the α values is therefore very difficult, one does not know if the behaviour originates from some real effect or from the limitations of the hard sphere approximation. The fact that $\alpha_{\text{II}} > \alpha_{\text{I}}$ for Pb, Au and Cu will be shown later to be due to the neglect of the contribution of the next collisions of the projectile to sputtering. The influence of the low binding energy of the Pb atoms is also visible in the high absolute value of α_{I} , compared with the Cu case for example. An incoming ion will transfer energy to a lattice atom, this lattice atom in turn will give its energy to other lattice atoms and so on. In this way a whole collision cascade is started. The number of cascade atoms in an energy interval $(E, E + \Delta E)$ is larger for lower energies (Sanders 1966). Therefore a cascade reaching a surface where the atoms are bound with low energies will eject more particles than in a case that the surface binding energy is high.

In this way a low binding energy leads to a high α value.

Further discussion of the α values is not very useful and we may conclude by saying that in spite of the very good description obtained with the theory of Odintsov it does not bring us any further with respect to questions like: what is the length of focusing collision ranges and at what depth are collisions of the incident particle still contributing to the sputtering process.

We will therefore try to do it in another way as will be treated in the next section.

4.3. THE INFLUENCE OF CHANNELING ON SINGLE CRYSTAL SPUTTERING

As seen in the preceding sections a good description of sputtering measurements in the keV region can be obtained with the hard sphere transparency theories. These theories neglect the possibility that after the first collision the projectile can make more collisions which eventually give rise to sputtering. The purpose of this section is to show that it is possible to describe sputtering ratio measurements using the theory of Lindhard for channeling of energetic ions in a crystal lattice. As said in chapter III the beam can be divided inside the crystal into two beams, whenever the incident beam is aligned within a certain critical angle $C \Psi_2$ ($1 < C < 2$) with the direction of a row of atoms. The two beams are an aligned and a random or nonaligned beam. The aligned beam experiences abnormal low energy losses, whereas the non aligned beam is equivalent to a beam in a random lattice. A comparison of Ψ_2 with the widths of the minima Ψ_w found for sputtering ratios of different f. c. c. crystals as a function of the angle of incidence, strongly suggests an effective influence of channeling on the sputtering phenomenon (Table V).

Furthermore the critical energy for channeling E_c (3.17) of Ar^+ in the [411] direction of a copper crystal is 10 keV. If one assumes that a channeled particle does not contribute to sputtering it follows directly that below the critical energy for channeling no minimum in the sputtering ratio will occur. This forms a simple explanation for the disappearance of the [411] minimum below 10 keV (see fig. 2.12). The assumption made in the preceding transparency theories that only collisions in the few top layers give rise to sputtering can therefore be replaced by the assumption that only particles which have collided in the few top layers are entering the random beam and transfer enough energy on their path through the crystal to cause sputtering. The other particles belong to the aligned beam and their contribution to the sputtering yield can in first approximation be neg-

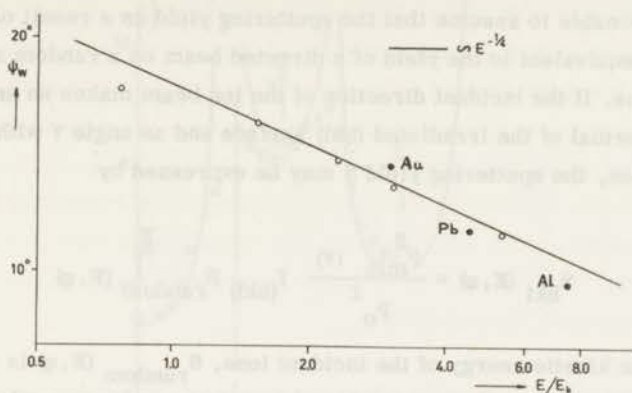


Fig. 4.7. The experimental widths of the $[100]$ -minima for Ar ions on a (100) crystal plotted against a reduced energy. The open circles are from 5-, 10-, 15-, 20- and 35 keV ions on Cu, the black dots are from 20 keV ions on Au, Pb and Al crystals. See also Table V.

$$E_k = 3aZ_1Z_2e^2/4\pi\epsilon_0d_{100}^3$$

Table V.

Comparison of Ψ_2 with the widths Ψ_w for sputtering ratios of different f.c.c. crystals as a function of the angle of incidence.

20 keV Ar ⁺	Ψ_w [100]	Ψ_2 [100]	Ψ_2/Ψ_w [100]	Ψ_w [211]	Ψ_2 [211]	Ψ_2/Ψ_w [211]
Cu	12° .9	7° .6	0.59	8° .7	6° .5	0.75
Au	13° .8	8° .2	0.59	8° .7	7° .0	0.80
Pb	11° .1	7° .0	0.63	7° .5	6° .0	0.80
Al	9° .6	6° .0	0.63	6° .6	5° .7	0.86
Ar ⁺ on Cu						
5 keV	17° .2	10° .7	0.63	11° .4	9° .1	0.80
10 keV	15° .6	9° .0	0.58	9° .8	8° .4	0.86
15 keV	14° .0	8° .2	0.59	8° .7	7° .0	0.80
20 keV	12° .9	7° .6	0.59	8° .7	6° .5	0.75
35 keV	11° .2	6° .6	0.59	6° .8	5° .6	0.82

lected. The equivalency of the random beam and a beam in a random lattice makes it reasonable to assume that the sputtering yield as a result of the random beam is equivalent to the yield of a directed beam on a random assembly of target atoms. If the incident direction of the ion beam makes an angle φ with the surface normal of the irradiated (hkl) surface and an angle Ψ with the closest string direction, the sputtering yield S may be expressed by

$$S_{\text{hkl}}(E, \varphi) = \frac{p_{\text{min}}^2(\Psi)}{p_0^2} f_{(\text{hkl})} S_{\text{random}}(E, \varphi) \quad (4.15)$$

where E is the kinetic energy of the incident ions, $S_{\text{random}}(E, \varphi)$ is the sputtering yield of a structureless assembly of target atoms for an angle of incidence φ and $p_{\text{min}}^2(\Psi)/p_0^2$ the probability that an incident ion will enter the random beam (see eq. 3.18). The "efficiency" factor $f_{(\text{hkl})}$ would be unity if the theory were exact and can be used to measure its deviation from observation. For the "random" yield $S_{\text{random}}(E, \varphi)$ one can use the experimental results on the sputtering of polycrystalline metals. For the calculated results given in fig. 4.8 and fig. 4.9, we used for $S_{\text{polycryst}}(E, 0^\circ)$ the measurements of Yonts and

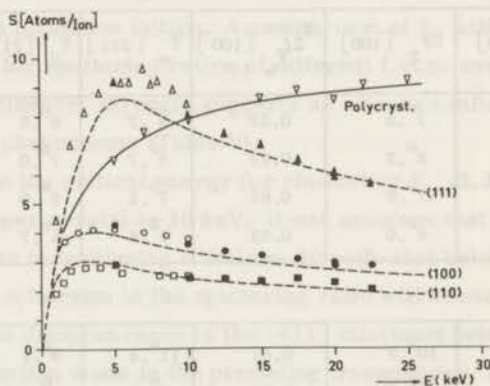


Fig. 4.8. The sputtering ratio as a function of the energy of normally incident Ar ions on different Cu monocrystals. The points are experimental, the broken curves have been calculated from the polycrystalline curve as measured by Yonts et al. (1960).

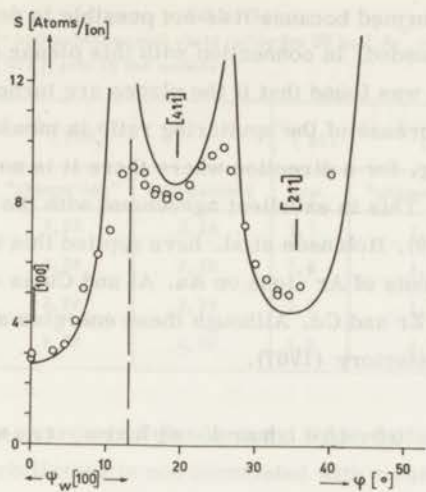


Fig. 4.9. The sputtering ratio for 20 keV Ar^+ ions on a (100) Cu crystal. The angle of incidence has been changed by rotating the crystal around a [011] axis in the surface. The points are experimental, the curve has been calculated according to formula (15).

assumed the angular behaviour to be given by $\cos^{-1} \varphi$. The efficiency factors $f_{(111)} = f_{(100)} = 1.3$ and $f_{(110)} = 1.6$ giving the best fit differ from unity for the following reasons: a) the random part of the beam always collides in the first layers; b) part of the ions impinging on a polycrystalline target will channel as well, c) the efficiency factor accounts for any orientation dependence of the ejection mechanism (such as for instance focusing along closepacked directions). As can be seen from the figures the fitting is quite good. The place of the maxima in the monocrystalline sputtering as a function of the incident energy is predicted well. The same can be said about the ratio of the predicted values in the minima. The predicted values between the minima are too high because in the calculation the occurrence of planar channeling is neglected. The crystal has been turned around a [011]-axis in the surface, this means that the incident beam is always parallel to the (011) planes perpendicular to the surface. Between such planes a similar effect as treated for low index directions, can lead to abnormal low energy losses of the incident beam. This so called, planar channeling becomes important as soon as the axial channeling is less probable. The inclusion of a probability for planar channeling in the calculation will give a decrease of the calculated sputtering yield for ψ close to $C \psi_2$. Such a calcula-

tion has not been performed because it is not possible to derive from Lindhard's theory the formulae needed. In connection with this planar channeling we refer to fig. 2.13, where it was found that if the planes are turned out from the beam direction a further increase of the sputtering ratio is measured. The highest value of the sputtering, for a direction where there is no channeling at all, was found to be 12.5. This is in excellent agreement with the predicted value at about 25° (see fig. 4.9). Robinson et al. have applied this model to 1-5 keV sputtering measurements of Ar^+ ions on Au, Al and Cu as well as on the hexagonal metals Mg, Zn, Zr and Cd. Although these energies are rather low, the results are quite satisfactory (1967).

4.3.1. Extension of the hard sphere transparency model.

It was demonstrated in the preceding section that a reasonable description of sputtering measurements can be obtained if one assumes that the sputtering is a result of the action of the random beam only. This means, in principle that more than one collision of the incident ion contributes to sputtering. It is therefore interesting to compare the predicted values in the minima in the "first collision" hard sphere transparency model and in the "channeling model".

According to the channeling model the sputtering ratios in the minima ($\Psi = 0$ in eq. 3.18 and 4.15) are given by $S_{[hkl]} \sim \frac{1}{\cos \varphi} d_{[hkl]}^{3/2}$ where $d_{[hkl]}$ is the string parameter of the $[hkl]$ direction. If we assume equal values for Odintsov's α 's the corresponding expression in the hard sphere transparency model reads: $S_{[hkl]} \sim \frac{1}{\cos \varphi} d_{[hkl]}$. This $d_{[hkl]}$ dependence can be compared with experiment by calculating the yield ratios of the $[411]$ -, $[211]$ - and $[100]$ direction at $\varphi = 19^\circ$, $\varphi = 35^\circ$ and $\varphi = 0^\circ$ respectively. (Table VI).

It can be seen that the experimental values fall just between the values calculated from both models. This means that in the channeling model the neglect of contribution of the first collision is not correct. In the first collision hard sphere transparency model the neglect of further collisions of the incident ion is certainly responsible for the strange behaviour of the α values (Table II). The fact that α_{II} is greater than α_I forms a compensation for the wrong $d_{[hkl]}$ dependence in the transparency model. This dependence however seems to be correct for the Al case. It can be concluded from the observed $d_{[hkl]}$ dependence that the sputtering is a result of the first collision ($\sim d_{[hkl]}$) and after that from a number of collisions of the random part of the beam ($\sim d_{[hkl]}^{3/2}$).

Table VI.

Comparison of calculated- and experimental yield ratios for 20 keV Ar⁺ ions on different (100) single crystals turned around a [011] axis in the surface.

20 keV Ar ⁺ ions on	S [411] / S [100]			S [211] / S [100]		
	exp.	"channeling"	transparency	exp.	"channeling"	transparency
Cu	2,8	3,28	2,26	1,7	1,64	1,49
Au	2,7	3,28	2,26	1,6	1,64	1,49
Pb	2,8	3,28	2,26	1,7	1,64	1,49
Al	2,1	3,28	2,26	1,5	1,64	1,49

This differs from the approach of Sanders and Onderdelinden (1966), where the contribution of next collisions is not correlated with a random beam concept (as defined by Lindhard); this means that the contribution of the next collisions has no d_{hkl} dependence. This together with the remarks made in chapter I, forms the reason that we do not use that description. It is furthermore hardly possible to extend the model to get a description of the angular measurements. A rough idea about the number of contributing collisions of the incident ion can be obtained in the following way. The contribution of the first collision can be given, according to the Odintsov description, by $\frac{1}{2} E_m \propto \pi R^2 / \pi p_o^2$. After the first collision only the random part of the beam contributes. This random part we say moves in a random lattice and its contribution to the sputtering can be given by the following analogous expression:

$$\frac{\pi p_{\min}^2}{\pi p_o^2} \cdot \sum_n \frac{\pi R_n^2}{(\pi p_o^2)_{\text{random}}} \quad \frac{1}{2} \alpha_n (E_m)_n, \text{ where the summation must be}$$

extended over the number of collisions of the incident ion still important for sputtering. A "collision" of the incident ion is thus defined as traversing a distance d_{random} , with $d_{\text{random}} = 2 N^{-1/3}$. If we assume that there is no spread in the energy loss, the expression for the energy E_m of the incident ion after n collisions reads (in the hard sphere model):

$$(E_m)_n \approx \frac{1}{2} E_m \left(1 - \frac{1}{2} \frac{\pi R^2}{(\pi p_o^2)_{\text{random}}} \right)^n, \text{ where the increase in the hard sphere}$$

radius R with decreasing energy is neglected. If we take $\alpha_n = \alpha$ the many-collision expression in the Odintsov notation becomes:

$$S_{[hkl]} = \frac{1}{2} \alpha E_m \frac{\pi R^2}{(\pi p_o^2)_{hkl}} \left[1 + \frac{1}{2} \frac{\pi p_{\min}^2}{(\pi p_o^2)_{\text{random}}} \sum_n \left(1 - \frac{1}{2} \frac{\pi R^2}{(\pi p_o^2)_{\text{random}}} \right)^n \right] \quad (16)$$

From this equation one can calculate the number of collisions of the incident ion still contributing to sputtering from the experimental ratio $S_{[411]}/S_{[100]}$. The results for different n values are shown in Table VII for different projectile energies on a copper (100) crystal. It may be remarked that for the calculation of the energy loss we used a hard sphere radius a factor 2.3 smaller than R_{Odintsov} (see section 4.2.1 and 4.2.2). From the calculations it follows that the prediction of the values in the minima for a fixed number of collisions is not bad. The best value, $n = 10$, means that if we count the next collisions with the same weight as the first collision the layer important for sputtering is about 40 Å for $d_{\text{random}} = 4,5 \text{ \AA}$.

Table VII.
Comparison of experimental values of $S_{[411]}/S_{[100]}$ with calculated results from equation (16), for Ar⁺ ions on a (100) Cu crystal.

E in keV		5	10	15	20	35
$\frac{S_{[411]}}{S_{[100]}}$	n = 20	2,32	3,04	3,01	2,98	2,92
	n = 15	2,32	2,99	2,95	2,93	2,86
	n = 10	2,31	2,91	2,87	2,84	2,77
	n = 5	2,30	2,75	2,71	2,66	2,60
experiment		2,4	2,9 ¹	2,8 ⁴	2,8 ²	2,6 ⁵

4.3.2. Description of the experimental results with a power potential.

The hard sphere model, used in the preceding section, is not the most adequate way to describe relatively low energy transfers between the incoming projectile and the target atoms. It is therefore better to construct a description with the aid of a more realistic potential model. It may be remarked here that Martynenko (1964) used the model of Odintsov (1963) to construct a first collision transparency theory with the aid of an r^{-2} potential. It is not possible however to

include in his model the idea that after the first collision there are more collisions (of the random beam) contributing to sputtering. We have the reversed situation for the theory of Brandt and Laubert (1967) for polycrystalline materials. In that case it is not possible to find an expression for the contribution of the first collision.

One might ask why we do not use the statistical calculations of Sanders (1967, 1968) as a basis for a description of our experimental results. These calculations give information on the following subjects: ranges of projectiles, number of low-energy recoils in a collision cascade and spatial extension of a collision cascade in amorphous material. In principle it is possible to derive from the spatial extension of a collision cascade the number of particles ejected. Sputtering however has to do with a relatively small tail of the collision cascade induced by the bombarding ion. It is obvious that varying assumptions affecting only slightly the bulk of the cascade may have a drastic influence on the tails (Sigmund 1968), especially for monocrystals. Another difficulty is formed by the fact that the influence of the lattice must be introduced for the incoming ions as well as for the low-energetic recoil atoms in the cascade. It was therefore hardly possible to derive sputtering ratio values from this work. We therefore preferred an extension of the rough model presented in the preceding section. We will give a description of our results based on the following assumptions: The sputtering ratio is proportional to the energy dissipation of the beam in a surface layer with thickness x_0 , where the energy dissipation of the aligned beam can be neglected.

The obtained description will therefore be a two parameter description. The parameters are the proportionality constant α and the thickness of the layer important for sputtering, x_0 . The problem is put in this form to get information about the influence of focusing collision ranges on x_0 values for different materials. To calculate the dissipated energy an r^{-3} potential is used. This potential (3.6) is in accord with the string potential used for the calculation of the critical angle Ψ_2 . The scattering cross-section for this potential (see 3.8) is

$$d\sigma_{12}(E, T) = B_{12} E^{-1/3} T^{-4/3} dT \quad (4.17)$$

where E is the energy of the incident particles and T the transferred energy. For the interaction of fast recoils with other target particles we use the constant B_{22} defined in a similar way.

To calculate the dissipated energy of the random beam it is again assumed that after the first collision this beam is equivalent to a beam on a random lattice.

The dissipated energy $F_{12}(E, x_0)$ of a normally incident beam on a random lattice within x_0 has been calculated from a recurrence relation. This recurrence relation is derived with the following assumptions:

- 1) the angular deviation of the projectile particles (1) traversing the distance x_0 in the target can be neglected;
- 2) the spread around the mean energy $\overline{E(x)}$ of projectiles at depth x is small enough to take $\overline{E(x)^n} \approx \overline{E(x)}^n$ for $\frac{1}{3} < n < 1$.

These approximations are not valid for low energies, where the projectile will lose nearly all its energy within x_0 . In this low energy region however, we simply have $F_{12}(E, x_0) \approx E$. For higher energies the approximation is not too poor because the scattering cross-section is strongly forward peaked, i. e. there is a relatively high probability for low energy transfers. The number of recoil particles with energy E_0 , dE_0 , created directly by the beam at depth x , Δx can be given by

$$N \Delta x d\sigma_{12}(\overline{E(x)}, E_0), \quad (4.18)$$

where N is the number density of the target.

These recoils are moving away from the region x , Δx in a direction making an angle with the x -direction. In view of assumption 1) this angle is given by $\cos\varphi = (E_0/E_m(x))^{1/2}$, where $\overline{E_m(x)} = C_{12} \overline{E(x)} = 4M_1 M_2 / (M_1 + M_2)^2 \overline{E(x)}$. The energy dissipation of these recoils within x_0 can be given by $F_{22}(E_0, (x_0 - x) / (E_0/E_m(x))^{1/2})$.

In this way we arrive at the following relation for $F_{12}(E, x_0)$:

$$F_{12}(E, x_0) = \int_0^{x_0} dx \int_0^{\overline{E_m(x)}} N d\sigma_{12}(\overline{E(x)}, E_0) \cdot F_{22}(E_0, (x_0 - x) / (E_0/E_m(x))^{1/2}) \quad (4.19)$$

By taking the projectile of the same species as the target particles an analogous equation is obtained for $F_{22}(E, x_0)$.

With the aid of equation (17) and assumptions 1) and 2) we find

$$\overline{E(x)} = (E^{2/3} - NB_{12} C_{12}^{2/3} x)^{3/2} \quad (4.20)$$

In finding a solution for equation (19) we take first the case of equal projectile and target atoms. As a boundary condition we have for low energies $F_{22}(E, x_0) \approx E$. This means that at low energies the sputtering ratio is proportional

to the energy of the incoming ions. We define an energy to be low if $E < E_{12} = (NB_{12} C_{12}^{2/3} x_o)^{3/2}$. For Ar^+ on copper and $x_o = 50 \text{ \AA}$ this means $E_{12} \approx 2 \text{ keV}$. This is not in contradiction with low energy sputtering measurements above threshold. Assuming that for high energies the solution can be given by a form like $E \left(\frac{NB_{22} x_o}{E^{2/3}} \right)^\epsilon$ one can find ϵ from equation (19) for equal particles. The function $F_{12}(E, x_o)$ for unlike particles follows from equation (19) by direct integration. An approximate solution of (19) for the entire region can be given by

$$F_{12}(E, x_o) = E \left\{ 1 - \exp - \left[(NB_{12} x_o E^{-2/3}) (NB_{22} C_{12}^{1/2} x_o E^{-2/3})^{4/7} \right] \right\} \quad (4.20)$$

The energy dissipation of an incident beam on a monocrystalline target follows from multiplication of (20) by the non-channeled fraction given by equation 3.18 plus the contribution of the first collision. This contribution can be derived from the results obtained above and reads:

$$F_{12 \text{ first collision}}(E, x_o) = \frac{1}{(\pi p_o^2)_{hkl}} \frac{3}{2} B_{12} C_{12}^{2/3} E^{1/3} \left\{ 1 - \exp - \right. \\ \left. + (2.2 NB_{22} x_o E_m^{-2/3})^{4/7} \right\}, \quad (4.21)$$

for a (hkl) crystal bombarded along the surface normal. If the incident beam has an angle φ with the surface normal x_o must be replaced by $x_o/\cos \varphi$. The sputtering ratio for an incident ion beam (1) on a target (2) can now be given by

$$S_{(hkl)}(E, \varphi) = \alpha_{(hkl)} \left\{ F_{12 \text{ first collision}}(E, x_o/\cos \varphi) + \frac{\pi p_{\min}^2(E, \varphi, (hkl))}{(\pi p_o^2)_{(hkl), \varphi}} \right. \\ \left. F_{12}(E, x_o/\cos \varphi) \right\} \quad (4.22)$$

where E is the energy of the incident ions, φ the angle of incidence with respect to the surface normal, $\pi p_{\min}^2 / \pi p_o^2$ is the non channeled fraction (3.18), (hkl) the orientation of the bombarded surface and $\alpha_{(hkl)}$ and x_o are the fitting parameters. The calculation has been performed for an Ar^+ , Cu^+ and Kr^+ ion beam normally incident on a (111)-, (110)- and (100) Cu single crystal in the energy range 1 - 40 keV. The appropriate numbers are given in table VIII. A fitting to the experimental ratios by the proportionality constant α is

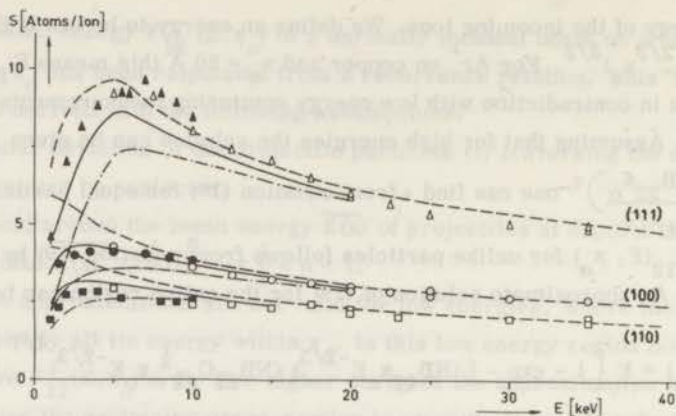


Fig. 4.10. Measured sputtering ratio as a function of the energy for normally incident Ar ions on different Cu crystals, compared with calculations according to equation (22).

- theoretical, $x_o = 30 \text{ \AA}$; $\alpha_{111} = 6.50$, $\alpha_{100} = 6.50$, $\alpha_{110} = 7.47 \text{ [keV}^{-1}\text{]}$
- theoretical, $x_o = 60 \text{ \AA}$; $\alpha_{111} = 2.78$, $\alpha_{100} = 2.88$, $\alpha_{110} = 3.38 \text{ [keV}^{-1}\text{]}$
- · - · - theoretical, $x_o = 90 \text{ \AA}$; $\alpha_{111} = 1.68$, $\alpha_{100} = 1.78$, $\alpha_{110} = 2.13 \text{ [keV}^{-1}\text{]}$

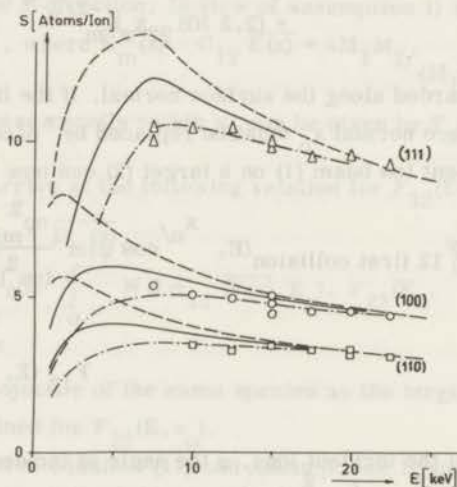


Fig. 4.11. Measured sputtering ratio as a function of the energy for normally incident Cu ions on different Cu crystals, compared with calculations according to equation (22).

- theoretical, $x_o = 30 \text{ \AA}$; $\alpha_{111} = 6.25$, $\alpha_{100} = 6.19$, $\alpha_{110} = 6.76 \text{ [keV}^{-1}\text{]}$
- theoretical, $x_o = 60 \text{ \AA}$; $\alpha_{111} = 2.67$, $\alpha_{100} = 2.74$, $\alpha_{110} = 3.05 \text{ [keV}^{-1}\text{]}$
- · - · - theoretical, $x_o = 90 \text{ \AA}$; $\alpha_{111} = 1.66$, $\alpha_{100} = 1.73$, $\alpha_{110} = 1.96 \text{ [keV}^{-1}\text{]}$

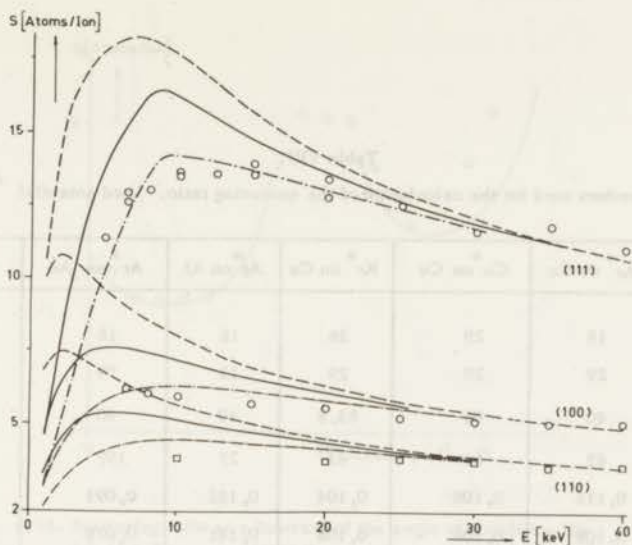


Fig. 4.12. Measured sputtering ratio as a function of the energy for normally incident Kr ions on different Cu crystals, compared with calculations according to equation(22).

- theoretical, $x_o = 30 \text{ \AA}$; $\alpha_{111} = 7.33$, $\alpha_{100} = 6.73$, $\alpha_{110} = 7.48 \text{ [keV}^{-1}\text{]}$
- theoretical, $x_o = 60 \text{ \AA}$; $\alpha_{111} = 3.07$, $\alpha_{100} = 2.92$, $\alpha_{110} = 3.33 \text{ [keV}^{-1}\text{]}$
- - - theoretical, $x_o = 90 \text{ \AA}$; $\alpha_{111} = 1.80$, $\alpha_{100} = 1.82$, $\alpha_{110} = 2.08 \text{ [keV}^{-1}\text{]}$

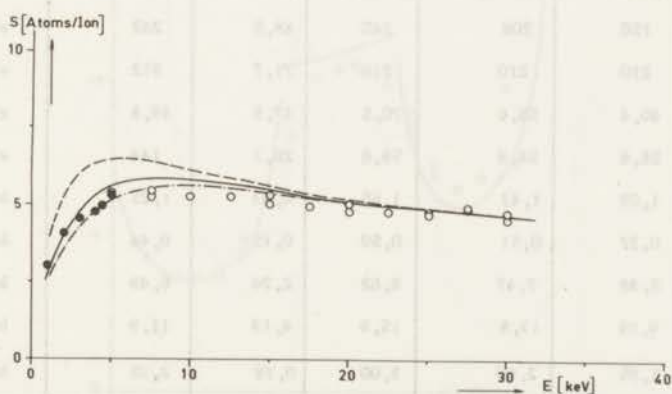


Fig. 4.13. Measured sputtering ratio as a function of the energy for normally incident Ar ions on a (100) Au crystal, compared with calculations. (equation (22)).

- theoretical, $x_o = 105 \text{ \AA}$; $\alpha_{100} = 3.16 \text{ [keV}^{-1}\text{]}$
- theoretical, $x_o = 135 \text{ \AA}$; $\alpha_{100} = 2.37 \text{ [keV}^{-1}\text{]}$
- - - theoretical, $x_o = 150 \text{ \AA}$; $\alpha_{100} = 2.10 \text{ [keV}^{-1}\text{]}$

Table VIII.

Some numbers used for the calculation of the sputtering ratio. Used potential $A_{12/3}^r$

	Ar ⁺ on Cu	Cu ⁺ on Cu	Kr ⁺ on Cu	Ar ⁺ on Al	Ar ⁺ on Au	units
Z ₁	18	29	36	18	18	
Z ₂	29	29	29	13	79	
M ₁	40	63	83,8	40	40	amu
M ₂	63	63	63	27	197	amu
a ₁₂	0,116	0,108	0,104	0,133	0,093	$\frac{\text{Å}}{\text{Å}}$
a ₂₂	0,108	0,108	0,108	0,141	0,078	$\frac{\text{Å}}{\text{Å}}$
C ₁₂	0,948	1,000	0,980	0,948	0,561	
d ₁₀₀	3,60	3,60	3,60	4,03	4,05	$\frac{\text{Å}}{\text{Å}}$
d ₁₁₀	2,55	2,55	2,55	2,85	2,87	$\frac{\text{Å}}{\text{Å}}$
d ₁₁₁	6,24	6,24	6,24	7,00	7,02	$\frac{\text{Å}}{\text{Å}}$
d ₄₁₁	7,64	7,64	7,64	8,55	8,60	$\frac{\text{Å}}{\text{Å}}$
d ₂₁₁	4,38	4,38	4,38	4,90	4,93	$\frac{\text{Å}}{\text{Å}}$
N	$8,65 \times 10^{-2}$	$8,65 \times 10^{-2}$	$8,65 \times 10^{-2}$	$6,15 \times 10^{-2}$	$6,02 \times 10^{-2}$	$\frac{\text{Å}^{-3}}{\text{Å}^{-3}}$
A ₁₂	150	208	240	88,5	262	$\text{eV} \frac{\text{Å}^3}{\text{Å}^3}$
A ₂₂	210	210	210	71,7	812	$\text{eV} \frac{\text{Å}^3}{\text{Å}^3}$
B ₁₂	40,4	58,6	70,5	37,5	39,8	$\text{eV} \frac{2/3 \text{Å}^2}{\text{Å}^2}$
B ₂₂	58,6	58,6	58,6	28,7	144	$\text{eV} \frac{2/3 \text{Å}^2}{\text{Å}^2}$
E _c (100)	1,03	1,43	1,65	0,43	1,25	keV
E _c (110)	0,37	0,51	0,59	0,15	0,44	keV
E _c (111)	5,38	7,47	8,62	2,26	6,49	keV
E _c (411)	9,93	13,8	15,9	4,13	11,9	keV
E _c (211)	1,95	2,60	3,00	0,78	2,25	keV

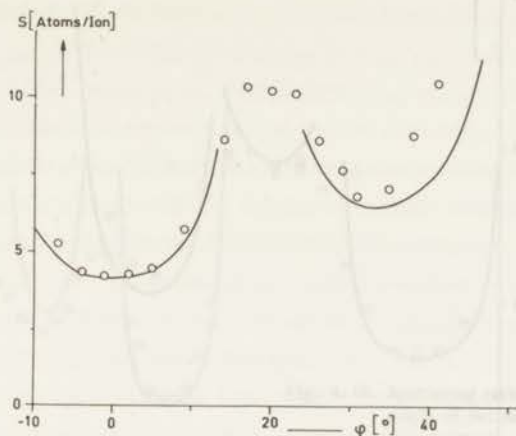


Fig. 4.14. Sputtering ratio as a function of the angle of incidence for 5 keV Ar^+ ions on a (100) Cu crystal turned around a $[011]$ axis. The points are experimental, the curves theoretical (equation (22)). Used parameters: $x_0 = 60 \text{ \AA}$, $\alpha_{100} = 2.81 \text{ keV}^{-1}$, $C = 1.2$.

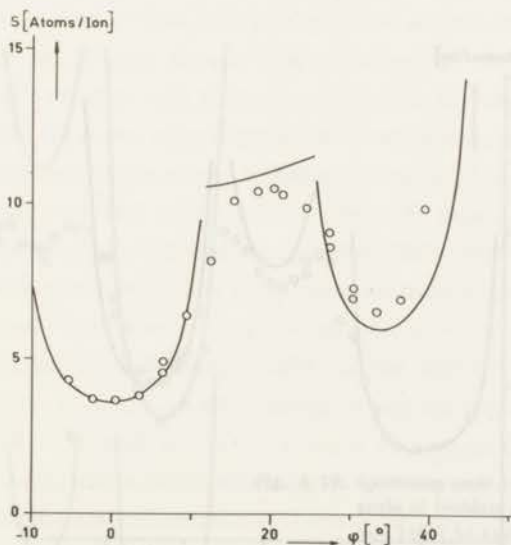


Fig. 4.15. Sputtering ratio as a function of the angle of incidence for 10 keV Ar^+ ions on a (100) Cu crystal turned around a $[011]$ axis. The points are experimental, the curves theoretical (equation (22)). Used parameters: $x_0 = 60 \text{ \AA}$, $\alpha_{100} = 2.83 \text{ keV}^{-1}$, $C = 1.2$.

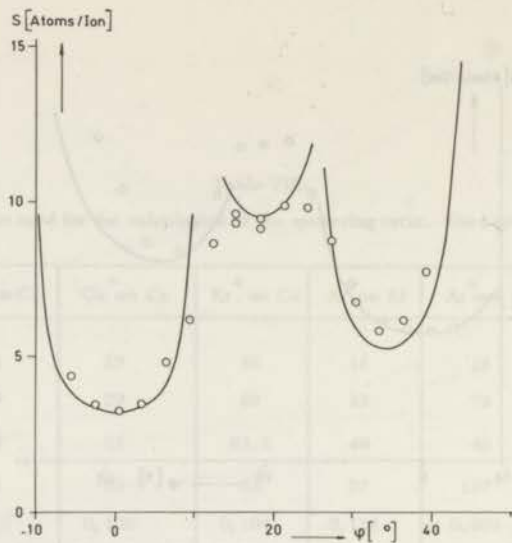


Fig. 4.16. Sputtering ratio as a function of the angle of incidence for 15 keV Ar^+ ions on a (100) Cu crystal turned around a [011] axis. The points are experimental, the curves theoretical (equation (22)). Used parameters: $x_{100} = 60 \text{ \AA}$, $\alpha_{100} = 2.76^\circ \text{ keV}^{-1}$, $C = 1.2$.

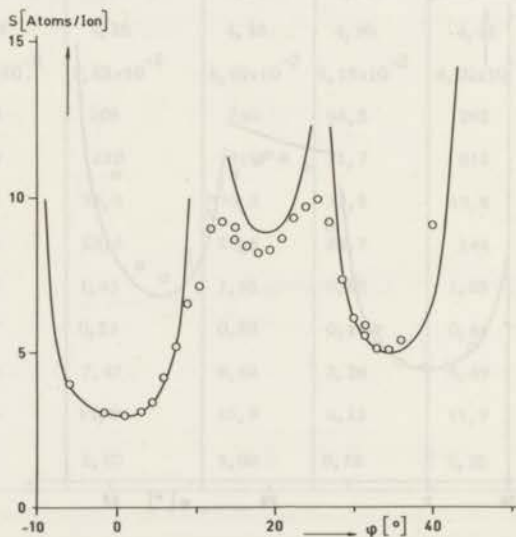


Fig. 4.17. Sputtering ratio as a function of the angle of incidence for 20 keV Ar^+ ions on a (100) Cu crystal turned around a [011] axis. The points are experimental, the curves theoretical (equation (22)). Used parameters: $x_{100} = 60 \text{ \AA}$, $\alpha_{100} = 2.83 \text{ keV}^{-1}$, $C = 1.2$.

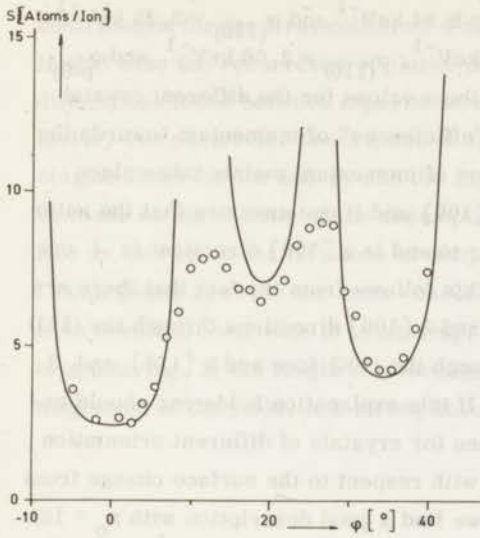


Fig. 4.18. Sputtering ratio as a function of the angle of incidence for 35 keV Ar⁺ ions on a (100) Cu crystal turned around a [011] axis. The points are experimental, the curves theoretical (equation (22)). Used parameters: $x_o = 60 \text{ \AA}$, $\alpha_{100} = 2.77 \text{ keV}^{-1}$, $C = 1.2$.

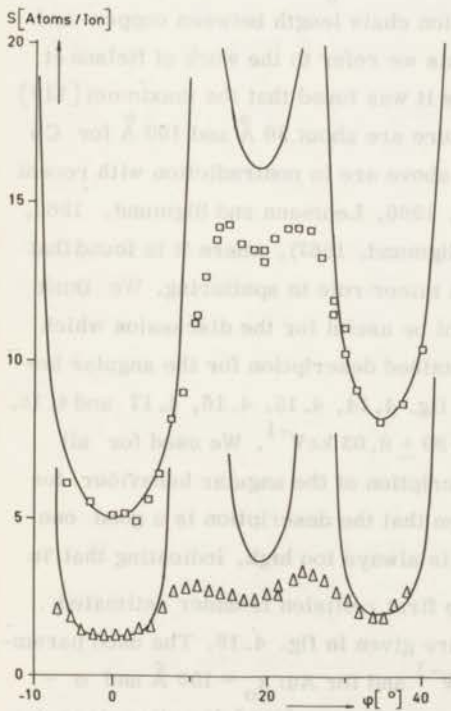


Fig. 4.19. Sputtering ratio as a function of the angle of incidence for 20 keV Ar⁺ ions on a (100) Au and a (100) Al crystal both turned around a [011] axis. The points are experimental, the curves theoretical (equation (22)). Used parameters: Al, $x_o = 60 \text{ \AA}$, $\alpha_{100} = 4.1 \text{ keV}^{-1}$, $C = 1.2$. Au, $x_o = 150 \text{ \AA}$, $\alpha_{100} = 2.08 \text{ keV}^{-1}$, $C = 1.2$.

shown in fig. 4.10, 4.11 and 4.12 for x_o values of 30, 60 and 90 Å. We found within 7% for $x_o = 60$ Å $\alpha_{(111)} = \alpha_{(100)} = 2,84 \text{ keV}^{-1}$ and $\alpha_{(110)} = 3,25 \text{ keV}^{-1}$ and for $x_o = 90$ Å $\alpha_{(111)} = \alpha_{(100)} = 1,75 \text{ keV}^{-1}$, $\alpha_{(110)} = 2,06 \text{ keV}^{-1}$ and $\alpha_{\text{poly-cryst.}} = 1,5 \text{ keV}^{-1}$. The differences in the α values for the different crystal faces may be due to different transport "efficiencies" of momentum towards the surface. If one assumes that the transport of momentum mainly takes place along the focusing directions [110] and [100] and if one assumes that the ratio of the probabilities to end in a [110] - or to end in a [100] direction is 4 one finds $\frac{\alpha_{(111)}}{\alpha_{(100)}} = 1$ and $\frac{\alpha_{(110)}}{\alpha_{(100)}} = 1,33$. This follows from the fact that there are 3 [110] and 3 [100] directions through the (111) face, 4 [110] and 1 [100] directions through the (100) face and 5 [110] and 2 [100] directions through the (110) face. If this explanation holds one should expect however also differences in x_o values for crystals of different orientation because the directions of different axes with respect to the surface change from crystal to crystal. For Ar^+ on (100) Au we find a good description with $x_o = 135$ Å and $\alpha_{(100)} = 1,4 \text{ keV}^{-1}$ and with $x_o = 150$ Å and $\alpha_{(100)} = 2,1 \text{ keV}^{-1}$ (fig. 4.13). So about the same α values as for the corresponding Ar-Cu case. The x_o values for gold are however considerably greater than the x_o values for copper indicating that the difference in focusing collision chain length between copper and gold does play a role. In connection with this we refer to the work of Nelson et al. (1962) and Sanders et al. (1964), where it was found that the maximum [110] focusing collision chains at room temperature are about 30 Å and 100 Å for Cu and Au respectively. The results obtained above are in contradiction with recent work of different authors (Harrison et al., 1966, Lehmann and Sigmund, 1966, Olson and Smith, 1966, 1967, Schulz and Sigmund, 1967), where it is found that the focused collision sequences only play a minor role in sputtering. We think however that the work presented here might be useful for the discussion which is still going on about this subject. The obtained description for the angular behaviour of the sputtering ratio is shown in fig. 4.14, 4.15, 4.16, 4.17 and 4.18. For Ar on Cu we used $x_o = 60$ Å and $\alpha = 2,80 \pm 0,03 \text{ keV}^{-1}$. We used for all curves $C = 1,2$. The sensitivity of the description of the angular behaviour for a change in x_o is very small. It can be seen that the description is a good one although the obtained ratio $S_{[411]}/S_{[100]}$ is always too high, indicating that in the model presented the contribution of the first collision is under estimated. The results for 20 keV Ar^+ on Au and Al are given in fig. 4.19. The used parameters are for Al: $x_o = 60$ Å and $\alpha = 4,1 \text{ keV}^{-1}$ and for Au: $x_o = 150$ Å and $\alpha = 2,1 \text{ keV}^{-1}$. The behaviour of the sputtering ratio at the [411] direction is not

predicted very well. The deviation for Au can be suppressed by taking a larger contribution for the first collision. For the Al case we have the same although in that case the occurrence of planar channeling can play a role. In spite of the differences found between experiment and theory we may conclude that a satisfactory two parameter description of sputtering ratio measurements has been obtained both for the energy and the angular behaviour. Further studies have to be made on the validity of the assumption of the perfectness of the crystal lattice as well as on the influence of temperature vibrations on the used model. I think (hope) however the main conclusions of this section, 1) a channeled particle does not contribute to sputtering, 2) not only the first collision contributes to sputtering, 3) the length of a focusing collision sequence is important for the magnitude of the yield, are strong enough to survive.

REFERENCES

- Abrahamson, A., 1963, Phys. Rev. 130, 693.
- Abrahamson, A. Hatcher, R. and Vineyard, G., 1960, Phys. Rev. 121, 159.
- Almén, O. and Bruce, G., 1961, Nucl. Instr. and Methods 11, 257.
- Anderson, G.H. and Wehner, G.K., 1960, J. Appl. Phys. 31, 2305.
- Anderson, H.H. and Sigmund, P., 1965, Risø Rep. N^o 103.
- Behrisch, R., 1964, Erg. ex. Natur Wissensch. 35, 295.
- Beuscher, H. and Kopitzki, K., 1965, Z. Phys. 184, 382.
- Bøgh, E., Davies, J.A. and Nielsen, K.O., 1964, Phys. Lett. 12, 129.
- Bohr, N., 1948, Kgl. Danske Videnskab Selskab, Mat. - Fys. Medd. 18, N^o 8.
- Born, M. and Mayer, J.E., 1932, Z. Phys. 75, 1.
- Brandt, W. and Laubert, R., 1967, Nucl. Instr. and Meth. 47, 201.
- Cobić, B. and Perović, B., 1959, Proc. IVth Int. Conf. Phen. Ion. Gases, Uppsala.
- Davies, J.A., Ball, G.C., Brown, F. and Domey, B., 1964, Can. J. Phys. 24, 1070; and references quoted there.
- Duesing, G. and Leibfried, G., 1965, Phys. Stat. Sol. 9, 463.
- Dupp, G. and Scharmann, A., 1966, Z. Phys. 194, 448.
- Erginsoy, C., 1964, Phys. Rev. Lett. 12, 366; 1965, Phys. Rev. Lett. 15, 360.
- Farmery, B.W., Nelson, R.S., Sizmann, R. and Thompson, M.W., 1965, Nucl. Instr. and Meth. 38, 231.
- Firsov, O.B., 1958, Soviet Phys. - JETP 6, 534.
- Fluit, J.M., 1963, Thesis, Leiden.
- Fluit, J.M., Rol, P.K. and Kistemaker, J., 1963, J. Appl. Phys. 34, 690.
- Fluit, J.M. and Rol, P.K., 1964, Physica 30, 857.
- Goldmann, D.T. and Simon, A., 1958, Phys. Rev. 109, 383.
- Gombas, P., 1949, "Die Statistische Theorie des Atoms", Springer, Vienna.
- Grönlund, F., and Moore, W.J., 1960, J. Chem. Phys. 32, 1540.
- Grove, W.R., 1852, Phil. Trans. Roy. Soc., 142, 87.
- Harrison, D.E., 1956, Phys. Rev. 102, 1473; 1957, Phys. Rev. 105, 1202; 1960, J. Chem. Phys. 32, 1336.
- Harrison, D.E., Johnson, J.P. and Levy, N.S., 1966, Appl. Phys. Lett. 8, 33.

- Hippel, A. von, 1926, *Ann. Phys.* 80, 672.
- Huntington, H.B., 1953, *Phys. Rev.* 91, 1092.
- Kaminski, M., 1965, *Struktur und Eigenschaften der Materie XXV*, Springer, Berlin - Heidelberg.
- Keywell, F., 1955, *Phys. Rev.* 97, 1611.
- Kingdon, K.H. and Langmuir, I., 1923, *Phys. Rev.* 22, 148.
- Koedam, M., 1959, *Physica* 25, 742; 1961, Thesis, Utrecht.
- Koedam, M. and Hoogendoorn, A., 1960, *Physica* 26, 351.
- Kopitzki, K. and Stier, H.E., 1961, *Z. Naturforsch.* 16 a, 1257; 1962, *Z. Naturforsch.* 17 a, 346.
- Lehmann, C., 1965, *Nucl. Instr. and Meth.* 38, 263.
- Lehmann, C. and Leibfried, G., 1963, *J. Appl. Phys.* 34, 2821.
- Lehmann, C. and Sigmund, P., 1966, *Phys. Stat. Sol.* 16, 507.
- Lindhard, J., 1965, *Kgl. Danske Videnskab Selskab, Mat.-Fys. Medd.* 34, N^o14.
- Lutz, H.O., Datz, S., Moak, C.D. and Noggle, T.S., 1966, *Phys. Rev. Lett.* 17, 285.
- Lutz, H.O. and Sizmann, R., 1964, *Z. Naturforsch.* 19 a, 1079.
- Magnuson, G.D. and Carlston, C.E., 1963, *J. Appl. Phys.* 34, 3267; 1965, *Phys. Rev.* 138, 759.
- Martynenko, Yu.V., 1965, *Soviet Phys. - Solid State* 6, 1581.
- Molchanov, V.A. and Chicherov, V.M., 1961, *Soviet Phys. - Doklady* 6, 222.
- Nelson, R.S., 1965, *Phil. Mag.* 11, 291; 1963, *Phil. Mag.* 8, 693.
- Nelson, R.S. and Thompson, M.W., 1963, *Phil. Mag.* 8, 1677. See also erratum in, 1964, *Phil. Mag.* 9, 1069.
- Nelson, R.S. and Thompson, M.W. and Montgomery, H., 1962, *Phil. Mag.* 7, 1385.
- Nielsen, K.O., 1956, "Electromagnetically Enriched Isotopes and Mass Spectrometry", Acad. Press, New York.
- Odintsov, D.D., 1963, *Soviet Phys. - Solid State* 5, 813.
- Olson, N.T., and Smith, H.P., 1966, *AIAA, J.* 4, 916; 1967, *Phys. Rev.* 157, 241.
- Onderdelinden, D., 1966, *Appl. Phys. Lett.* 8, 189.
- Onderdelinden, D., Saris, F.W. and Rol, P.K., 1966, *Proc. VIIIth Int. Conf. Phen. Ion. Gases*, Beograd.
- Patterson, H. and Tomlin, D.H., 1962, *Proc. Roy. Soc.* 265, 474.
- Pease, R.S., 1960, *Nuov. Cim. Suppl.* XIII.
- Penning, F.M. and Moubis, J.H.A., 1940, *Kon. Ned. Acad. Wetensch. Proc.* 43, 41.
- Perović, B. and Cobić B., 1961, *Proc. Vth Int. Conf. Phen. Ion. Gases*, Munich.
- Robinson, M.T., 1964, *Symp. on Atomic Collision Cascades in Radiation Damage*, Harwell; 1963, ORNL - 3493

- Robinson, M.T. and Oen, O.S., 1963, Phys. Rev. 132, 2385.
- Robinson, M.T. and Southern, A.L., 1967, J. Appl. Phys. 38, 2969.
- Rol., P.K., 1960, Thesis, Amsterdam.
- Rol., P.K., Fluit, J.M. and Kistemaker, J., 1957, Terzo Congr. Int. sui fenomeni d'ionizzazione nei Gas. Soc. It. di Fis 872; 1960, Physica 26, 1000.
- Rol., P.K., Fluit, J.M., Viehbock, F.P. and Jong, M. de, 1959, Proc. IVth Int. Conf. Phen. Ion. Gases, Uppsala.
- Sanders, J.B., 1966, Physica 32, 2197; 1967, Conf. on Atomic Collision and Penetration Studies with Energetic (keV) Ion Beams, Chalk River; 1968, Thesis, Leiden.
- Sanders, J.B. and Fluit, J.M., 1964, Physica 30, 129.
- Sanders, J.B. and Onderdelinden, D., 1966, Prov. VIIIth Int. Conf. Phen. Ion. Gases, Beograd.
- Schulz, F. and Sizmann, R., 1967, Proc. VIIIth Int. Conf. Phen. Ion. Gases, Vienna.
- Sigmund, P., 1967, Conf. on Atomic Collision and Penetration Studies with Energetic (keV) Ion Beams, Chalk River.
- Silsbee, R.H., 1957, J. Appl. 28, 1246.
- Snouse, T.W. and Haughney, L.C., 1966, J. Appl. Phys. 37, 700.
- Southern, A.L., Willis, W.R. and Robinson, M.T., 1963, J. Appl. Phys. 34, 153.
- Stuart, R.V., and Wehner, G.K., 1962, J. Appl. Phys. 33, 2345; 1964, J. Appl. Phys. 35, 1819.
- Tegart, W.J. McG., 1959, The Electrochemical and Chemical Polishing of Metals, Pergamon Press, London.
- Thompson, M.W., 1961, Coll. Int. Centre Nat. Rech. Sci., "Le Bombardement Ionique", Bellevue; 1963, Phys. Lett. 6, 24; 1964, Phys. Rev. Lett. 13, 756; 1961, Proc. Vth Int. Conf. Phen. Ion. Gases, Munich.
- Thompson, M.W. and Nelson, R.S., 1962, Phil. Mag. 7, 2015.
- Townes, C.H., 1944, Phys. Rev. 65, 319.
- Viehböck, F.P., Formann, E. and Wotke, H., 1967, Conf. on Atomic Collision and Penetration Studies with Energetic (keV) Ion. Beams, Chalk River.
- Wehner, G.K., 1955, Adv. in Electronic and Electron Physics VII, Acad. Press, New York; 1957, Phys. Rev. 102, 690; 1957, Phys. Rev. 108, 35; 1959, Phys. Rev. 114, 1270.
- Wehner, G.K. and Rosenberg, D., 1960, J. Appl. Phys. 31, 177.
- Weysenfeld, C.H., 1965, Proc. VIIIth Int. Conf. Phen. Ion. Gases, Beograd; 1966, Thesis, Utrecht.
- Yonts, O.C., Normand, C.E. and Harrison, D.E., 1960, J. Appl. Phys. 31, 447.
- Yurasova, V.E., Pleshivtsev and Orfanov, I.V., 1960, Soviet Phys. - JETP 37 (10), 689.
- Zilverschoon, C.J., 1954, Thesis, Amsterdam.

SUMMARY

This thesis deals with the sputtering of f. c. c. metals under keV ion bombardment. Experiments are performed to determine the sputtering ratio, i. e. the number of particles ejected per incoming ion. The sputtering ratio depends on the energy transfer of the ions to the metal atoms and on the transport of momentum towards the surface. Both effects are strongly influenced by the regular structure of the lattice. This thesis describes an investigation of the influence of the lattice structure on the energy transfer of the incoming ions. The measurements therefore have been compared with the so-called transparency theories, demonstrating some imperfections of these models. A more realistic treatment turns out to be possible with the aid of the theory of Lindhard on channeling of energetic ions in a lattice.

In Chapter I the typical dependence of the sputtering ratio on parameters like energy, mass and angle of incidence of the incoming ions is shown. Furthermore a short discussion of the theoretical work on sputtering is given.

In Chapter II the different effects which may influence the measurements are discussed. The error in the obtained sputtering ratios is estimated to be smaller than 3%.

The experimental results are given in the second part of Chapter II. Both the energy dependence and the angular dependence of the sputtering ratio are shown for various ions incident on single crystals of copper, gold, lead and aluminium. Maxima in the curves, giving the energy dependence for normally incident ions, shift towards higher energies for heavier ions, in accord with the result for polycrystalline materials. The width of the minima around the "open" crystal directions are shown to be energy dependent ($\sim E^{-\frac{1}{4}}$).

In Chapter III a short discussion is given on interaction potentials, which can be used for the calculation of the energy transfer of the incoming ions to the

target atoms. For the power potential used in Chapter IV a differential scattering cross-section has been derived with the aid of the momentum approximation.

The transport of momentum along a close-packed row of atoms is demonstrated in the hard sphere approximation. These "focused" collision sequences form an explanation for the preferential ejection directions of sputtered atoms. The purpose of this thesis however is an investigation of the influence of correlated collisions of the incoming ions on the sputtering ratio. Therefore a more extensive treatment of channeling of the incident ions is given. Formulae used in Chapter IV are derived from the theory of Lindhard on the influence of crystal lattice on motion of energetic charged particles.

Chapter IV deals with various models which can be used for the description of our experimental data. Transparency theories of different authors are given. A description of the measured sputtering ratio as a function of the angle of incidence has been obtained with the theory of Odintsov. Imperfections of the model are discussed.

A comparison of the energy behaviour of the widths of the minima found for the sputtering ratio as a function of the angle of incidence and the critical angle for channeling strongly suggests the idea that a channeled particle does not contribute to sputtering. This is sustained by the obtained description of the monocrystalline sputtering data from the corresponding polycrystalline results. The introduction of channeling leads to a more-collision hard-sphere transparency model showing that for an Ar^+ ion in the keV energy region incident on a copper crystal about ten collisions of the incident particle contribute to the sputtering. A more realistic treatment is obtained by the introduction of a power potential for the interaction of the incident ions and the target atoms. In this way a description of our experimental data has been obtained based on the following assumptions: the sputtering ratio is proportional to the energy dissipation of the incident beam in a surface layer with thickness x_0 ; the channeled part of the beam does not contribute to sputtering. The value of x_0 is found to be about 80 \AA for a copper target and 150 \AA for a gold target.

S A M E N V A T T I N G

Dit proefschrift handelt over de verstuiving van kubisch vlakgecentreerde metaalkristallen door bombardement met ionen in het keV-energiegebied. Experimenten zijn uitgevoerd ter bepaling van de verstuivingsverhouding, dit is het aantal uit het metaal gestoten atomen per inkomend ion. De grootte van de verstuivingsverhouding wordt enerzijds bepaald door de energie-overdracht van de ionen aan de metaalatomen en anderzijds door het transport van impuls naar het oppervlak. Beide effecten worden in sterke mate beïnvloed door de regelmatige opbouw van het metaalrooster. Dit proefschrift beschrijft een onderzoek naar de grootte van de roosterinvloed op de energie afgifte van de invallende ionen. De metingen worden daartoe vergeleken met de zogenaamde transparantie theorieën, waarbij enkele onvolkomenheden van deze modellen aan het licht komen. Een realistischer benadering blijkt mogelijk met behulp van de theorie van Lindhard over geleiding van ionen in de kanalen van het metaalrooster ("channeling").

In Hoofdstuk I wordt de afhankelijkheid van de verstuivingsverhouding getoond van parameters als energie, massa en hoek van inval van het projectiel. Verder wordt een kort overzicht van het theoretisch werk over verstuiving gegeven.

In Hoofdstuk II worden de verschillende effecten die de metingen kunnen beïnvloeden, behandeld. De fout in de verkregen verstuivingsverhoudingen wordt geschat kleiner dan 3% te zijn.

De experimentele resultaten worden in het tweede gedeelte van Hoofdstuk II gegeven. De afhankelijkheid van de verstuivingsverhouding van de energie en de hoek van inval wordt getoond voor verschillende soorten ionen op éénkristallen van koper, goud, lood en aluminium. De maxima, die optreden in de krommen die de energie afhankelijkheid voor loodrecht invallende ionen geven, ver-

schuiven naar hogere energieën voor ionen met hogere massa. Dit resultaat is in overeenstemming met eerdere resultaten voor polykristallijn materiaal. De breedte van de minima die optreden rond de "open"-kristalrichtingen in de krommen die de hoekafhankelijkheid geven, blijkt energie afhankelijk te zijn ($\sim E^{-\frac{1}{2}}$).

In Hoofdstuk III wordt een korte discussie gegeven over wisselwerkingspotentialen die gebruikt kunnen worden voor de berekening van de energieoverdracht van de invallende ionen aan de metaalatomen. Voor de uiteindelijk gebruikte machtpotentialen wordt een differentiële botsingsdoorsnede afgeleid.

Het transport van impuls langs een dichtgepakte rij atomen wordt gedemonstreerd met behulp van de harde bollen benadering. Deze "focuserende" stotenseries geven een verklaring voor het optreden van voorkeursuittreedrichtingen voor verstoven atomen. Het doel van dit proefschrift is echter het onderzoek naar de invloed van het optreden van gecorrleerde botsingen van de invallende ionen op de grootte van de verstuiwingsverhouding. Een uitgebreide behandeling van deze kanaalgeleiding is daarom noodzakelijk. Formules die gebruikt worden in Hoofdstuk IV, worden afgeleid met behulp van de theorie van Lindhard over de invloed van het kristalrooster op de beweging van energetische deeltjes.

Hoofdstuk IV behandelt verschillende modellen die gebruikt kunnen worden voor de beschrijving van onze meetresultaten. Transparantie theorieën van verscheidene auteurs worden gegeven. Een beschrijving van de gemeten verstuiwingsverhouding als functie van de hoek van inval der ionen is verkregen met de theorie van Odintsov. Onvolkomenheden van het model worden gediscussieerd.

Een vergelijking van de energieafhankelijkheid van de breedte der minima in de verstuiwingsverhouding als functie van de hoek van inval en de kritische hoek van kanaalgeleiding suggereert de idee dat een "gekanaliseerd" deeltje niet bijdraagt tot de verstuiwing. Dit wordt ondersteund door de verkregen beschrijving van de éénkristallijne verstuiwingsresultaten uit de corresponderende polykristallijne resultaten. De invoering van de kanaalgeleiding leidt tot een harde-bollen transparantie model, waarbij meer dan één botsing van het inkomende ion in rekening wordt gebracht. Er wordt aangetoond dat voor Ar^+ ionen met keV energieën opvallend op een koperkristal ongeveer 10 botsingen van het Ar^+ ion bijdragen aan de verstuiwing. Een realistischer beeld wordt verkregen door de invoering van een machtpotentiaal voor de interactie van de invallende ionen en de doelwit atomen. Op deze wijze wordt een beschrijving van onze meetresultaten verkregen gebaseerd op de volgende veronderstellingen: de ver-

DANKWOORD

Bij het gereedkomen van dit proefschrift wil ik gaarne dank brengen aan allen, die hebben meegewerkt aan het tot stand komen van dit proefschrift.

Ik denk hierbij in de eerste plaats aan dr P.K. Rol. Zijn leiding, vooral in de beginfase, is van het grootste belang geweest voor de keuze van de experimenten en de totstandkoming van het onderzoek. Met genoegen denk ik terug aan de vele discussies die wij samen hebben gevoerd. Dr J. Los wil ik bedanken voor het kritische doorlezen van het manuscript.

De gedachtewisseling en de samenwerking met de leden van de sputtergroep hebben het werk aan de experimenten aanzienlijk veraangenaamd. Gedurende een groot gedeelte van het onderzoek zijn drs F.W. Saris, W.L. Kroon en H.H. Kersten mijn directe medewerkers geweest. De samenwerking met hen is onmisbaar geweest voor de totstandkoming van dit proefschrift. De vele discussies met drs W.F. van der Weg, dr J.B. Sanders en drs J.J.P. Elich hebben in niet geringe mate bijgedragen tot een beter begrip van de experimentele resultaten.

De hulp van drs D.J. Bierman en H.H. Roukens bij het uitvoeren van de noodzakelijke berekeningen mag zeker niet onvermeld blijven.

Bij de constructie van het apparaat heb ik veel te danken gehad aan de constructeurs M.J. Hogervorst en E. de Haas en aan de instrumentmakerij onder leiding van A.F. Neuteboom.

Ik wil, tot slot, niet nalaten mijn erkentelijkheid te betuigen aan hen, die aan het proefschrift zelf een groot aandeel hebben gehad: Mej. M.J. Benavente voor het vervaardigen van de tekeningen, F.L. Monterie en Th. van Dijk voor het fotografisch werk, Mevr. G.H. Kingma, Mej. J.M. de Vletter en Mevr. C.A. Strout voor het typen van het manuscript en Mej. A. Klapmuts voor de hulp bij administratieve problemen.

